SIMULATION OF DRY ETCHED LINE - EDGE PROFILES

by

John L. Reynolds

Memorandum No. UCB/ERL M81/2

12 January 1981

ELECTRONICS RESEARCH LABORATORY

College of Engineering
University of California, Berkeley
94720

Research sponsored by the National Science Foundation under Grant ECS77-14600-A01, Hughes Aircraft, INTEL, Signetics, Hewlett-Packard and IBM Corporation.

ABSTRACT

Computer simulation of plasma etched two-dimensional profiles is explored. The model divides the process into three rate components: isotropic or chemically reactive etching, anisotropic or directional etching, and orientationally dependent ion beam etching. The algorithm extends the user-oriented computer program for Simulation And Modelling of Profiles in Lithography and Etching (SAMPLE) which simulates the time evolution of line-edge profiles by advancing nodes on a string. Applications here include residue left at a step using anisotropic etching and undercut produced using arsenic implanted poly-silicon layers.

The reported research completed the author's Master of Science Degree requirements for the University of California at Berkeley, December 1979. Although it is not an official copy, this has been reproduced using the UNIX work processor TROFF.

TABLE OF CONTENTS

I. Introduction.

As device sizes shrink etched profiles and shapes become increasingly important in IC fabrication. Dry etching techniques are particularly popular in producing small dimensions that achieve VLSI technologies. They range from chemical, isotropic processes, using tunnel or barrel reactors, to directional, physical processes, in diode or sputter etching systems. The variety affords anisotropy in etching for optimal profile control and pattern transfer. By adjusting rates within the range, computer simulation of the time evolution of line edge profiles is an especially useful tool in exploring and understanding various degrees of anisotropic dry etching processes.

Numerical algorithms suitable for simulating ion milled and sputtered profiles are reported by Carter et. al. [13,14,15] and Ducommun et al. [24,25]. Lehmann [40] and Bayly [5] report the modelling of other mechanisms in ion milling. Mathematical expressions describing simple linear profile features in anisotropic etching are given by Jinno and Inomata [39] and Cantagrel [12]. The case of reactive ion etching is considered in a cell dissolution model by Viswanathan[73].

This report generalizes a string development model [33,51] to the case of anisotropic dry etching. The algorithm is intended for use in the user oriented program for Simulation And Modelling of Profiles in Lithography and Etching (SAMPLE) [52,54]. The initial version of SAMPLE simulates the exposure and development of positive photoresists [53]. The routines reported here extend the capability to two-dimensional etched structures. They are applicable to dry etching processes as those reported by Mogab and Harshbarger[49], Schwartz et al. [64,65], and Coburn and Winters[21,22]. Basically, the routines divide the dry etching process into isotropic and anisotropic components. Each component is characterized by empirical etchrate information.

Section II discusses the various types of etching techniques and mechanisms involved. Section III describes the implementation of the string development model in dry etching. A few examples are presented for comparison in section IV and further exploratory studies are considered in V. Finally, the appendices explain the use of the etch routines, and their internal code.

TABLE I: ETCHING CHARACTERISTICS				
	Wet Chemical	Plasma	Reactive Ion	Ion Milling
Mask				
-				
thickness	...	...	depends on etchrates	depends on etchrates
adhesion	crucial	...	...	...
profile	...	...	depends on etchrates	critical in faceting
Substrate				
-				
overetch	undercut	undercut	flexible	substantial resist erosion
profile	circular cross section	$>45^{o}$	controllable	controllable
lines vs spaces	lines narrow	lines narrow	lines narrow slightly	lines vary with resist
selectivity	good	good	controllable	very poor
Operating Conditions				
-				
chamber	bath	barrel reactor	parallel plate reactor	ion mill or sputterer
power	none	<100W	100-300W	>200W
pressure	none	.1-20T	10-100mT	.2-20mT
temperature	varies	sensitive	sensitive	must be cooled
etchant	liquid	free radicals in plasma	free radicals and ions in plasma	ions (usually inert)

II. Theory.

First, a distinction is made among the different etching techniques referred to in this report. The techniques are divided into four categories; wet chemical, simple plasma etching, plasma assisted or reactive ion etching, and sputtering or ion milling. Table I. summarizes the characteristics of these processes.

In wet etching and simple plasma etching the substrate is immersed in a fluid (liquid or gas) which chemically reacts with the exposed surface. In wet etching, the liquid attacks the surface and soluble products are removed. Similarly, in dry etching, because only free radicals are present, the chemical nature dominates. The reaction produces volatile by-products which are removed by a vacuum pump. Physical reactions do not take place. A barrel plasma reactor achieves such conditions, usually at low powers and moderate pressures. Due to the chemical reaction, profiles develop isotropically with undercut of the mask and circular cross sections.

"Plasma assisted"[49] or reactive ion etching [9] is a combination of chemical and physical reactions. Ions are present in the plasma and are accelerated by an electric field. This radiation bombarding the surface enhances etching by speeding the chemical reaction and removing residue [49,68]. The added physical interaction allows etching to be anisotropic, primarily in the direction of the radiation flux. This reduces undercutting and allows more profile control. Planar systems operated at moderate power and low pressure demonstrate this type of etching.

At the physical extreme of etching there are sputtering and ion milling. Inert accelerated ions (e.g. Ar^+) physically remove chunks of the exposed material [8,11]. This leads to steep sidewalls, faceting and surface damage. To achieve useful etchrates with such a process, it must be carried out at very low pressures with the ions accelerated through extremely high electric fields. In ion milling, the ions are neutralized before striking the substrate. The neutralization distinguishes it from sputter etching and allows orientational flexibility since the substrate is not an electrode.

Consider, for example, the development of a silicon layer being plasma etched in a fluorine source, such as CF_4 or SF_6[10]. The basic reaction is:

$$Si + 4F \dashrightarrow SiF_4$$

In a barrel reactor, all ions are electrically shielded so that only free fluorine radicals are present. The etching then proceeds isotropically, wherever there is exposed silicon, fluorine is absorbed and silicon tetrafluoride removed by vacuum pumping. Any elements from the plasma that redeposit slow the etchrate without interrupting the isotropic behaviour. Similar isotropic etching conditions apply to other combinations of etchgas and samples. Surface area and loading effects may make the etch rate nonuniform, but these effects are considered locally secondary. Isotropic etching is identical to wet etching with ideal mask adhesion, too.

In the case of plasma assisted etching several mechanisms contribute to etching. First, due to the chemistry of the plasma discharge some isotropic etching will occur. A more important mechanism, ions in the discharge enhance etching in the direction of the electric field lines. Consider Figure 1, for the radiation flux shown, V_a is the purely chemical background etchrate and V_b is the physically enhanced rate. The energetic particles striking the surface

remove rate limiting residue and also speed any chemical reaction. The ratio:

$$A = \frac{V_b}{V_a + V_b}$$

defines a measure of the anisotropy. For A = 0 the process is completely isotropic with circular profiles, and for A = 1 the process is anisotropic yielding vertical sidewalls.

The enhancement of the etchrate by radiation allows a directionality in etching (see Figure 2). An orientation or angular dependence is then representative of reactive ion etching. The normal incident rate (i.e. in the flux's direction) is the largest, diminishing to zero at glancing incidence. This is effectively modelled as a cosine angular dependence (unlike the more complicated sputter etching with faceting angles and maxima away from normal incidence).

The third mechanism or ion effect is shadowing. Again, only the background, isotropic (V_a) etching is apparent in shadowed or unexposed areas, no matter what the orientation. This mechanism occurs most often while etching non-uniform surfaces at oblique angles of incidence.

Ion milling and sputtering require consideration of etchrates that have a more complicated orientational dependence than the simple cosine angular dependence [5,12]. The sputtering yield, the amount of material removed per second versus angle [11], is non-monotonic. This dependence leads to faceting and orientational preferred etching. Each material has a different sputtering yield angular dependence. In general, an analytic sputtering function can be used to determine an angular dependent etchrate [15,24]. This etchrate and local angular information is used to model the sputter etching of a line edge profile.

In this discussion, we have ignored secondary effects such as redeposition, rebounding, trenching, and surface limited etching that occur in more physical types of etching.

III. IMPLEMENTATION.

The next step is to build these characteristic etching components into a simulation algorithm. The algorithm, in this case, is intended for use in the user oriented program for Simulation And Modelling of Profiles in Lithography and Etching (SAMPLE [50,53,54]). The original model [33] advances nodes along a string to simulate the time evolution of a two dimensional profile. The simulation follows the exposure and development of positive photoresist, using stored rate information to determine the advancement of the string points. Similarly, the goal for the etching routines is to use rate information to advance the string nodes to simulate dry etching processes.

The plasma etching process is divided into two adjustable components; isotropic and anisotropic, each characterized by empirical etch rates, V_a and V_b, defined in Figure 1. The isotropic component V_a models, for example, a chemically reactive etch which results in profiles with undercut and circular cross sections. The anisotropic component V_a contains a directional dependence and shadowing effect caused by the more physical, ion-enhanced effects

in dry etching.

A piecewise linear string of points represents the two-dimensional line edge profile. The rate of advancement, or etch rate, of these points depends on their position and orientation. Figure 4 shows a magnified segment of the string model. Under isotropic conditions, the string-points are advanced at a constant rate V_0, in the direction of the perpendicular bisector of the adjacent segments. To model the directional mechanism in reactive ion etching, points are advanced in the direction of the radiation flux or electric field lines. A direction vector is calculated from the angular information and a specialized rate advances the string points along this unit vector, similar to the isotropic advancement. Alternatively, the anisotropic etchrate can be looked at as a rate proportional to the cosine of the angle between flux direction and the surface normal (the perpendicular bisector of adjacent segments). Both ways are equivalent to etching according to the etchant flux that would strike the exposed surface.

To incorporate the shadowing mechanism, the positions of all points are considered with respect to a line parallel to the radiation flux. Points that are shaded by other segments are advanced with only the isotropic, background rate. Hence, two adjustable rates and the internal shadowing calculation simulate the three mechanisms described in dry etching.

The user specifies the etchrates in plasma etching directly for simulation purposes. For each layer, a single rate is interpreted as the isotropic chemical component, while a second rate (if specified) is taken as V_b, the directional etch rate. The degree of anisotropy can be controlled by adjusting their ratio. When using directional etching, the incident flux direction is specified by an angle, which is assumed to be 0^o (normal incidence) if unspecified. The user inputs a single time, or a time range with a number of outputs, for etching durations. The layered structure is modelled by arranging and naming material layers with thicknesses in microns. The etching simulation can follow the lithographic routines directly, or a piecewise linear profile may be created and etching continued from it.

The ion milling or sputtering process is defined by a single, more complicated component. It uses the same advancing algorithm and shadowing mechanism as directional etching. In addition, average angular information is taken from adjacent segments and the incident ion beam. The simulation uses this information to determine a rate according to the sputtering yield [24,13,42,69]

$$S(\theta) = S_0(\phi/\rho)[A\cos\theta + B\cos^2\theta + C\cos^4\theta]$$

where S_0, A, B, and C characterize the sputtering yield of the material being ion etched. ρ is the atomic density of the layer and ϕ is the current density of the ion flux. Faceting is automatic due to the maximum etch rate at the facet angle.

The ion milling etch rates and durations are specified similar to those in dry etching. Also, an ion flux density is specified along with the angle of incidence. Analytics, A,B,C, are specified along with other material parameters for each layer when simulating ion milling.

In addition to the advancement, rate and shadowing subroutines, the model implements checking and delooping routines to manage the string [53]. Subroutine CHKR sees that the points remain equitably spaced along the string; deleting points that come too close, and adding points where segments advance apart. Subroutine DELOOP eliminates loops in the string if it

should cross itself during advancement.

There are also input routines for setting the initial line-edge profile (STPRFL) and or continuing from a developed profile (COMPAT). Output routines include a message and error subroutine (ETHMSG), a plotting subroutine (PLTLPR), a numerical printing routine (PRTNUM), and a card punching routine (PLTDGT) with coordinates of the string points.

Figure 7 illustrates the individual etching components and the output format of the two dimensional profile. In a). a nonerodible squared mask protects the isotropically etched substrate at three different times in the etching process. The previously defined anisotropic ratio A is 0. Characteristically the profile shows undercut and quartercircular cross sections. Beginning with the same profile Figure 7b). shows the profiles of a completely directionally etched substrate, A = 1, at the same three times. Here there is no undercutting and a vertical sidewall. In general an etching process is a combination of these two specified components. In Figure 7c). the substrate is etched with a 50% mixture of the two, that is A = 1/2.

IV. COMPARISON OF SIMULATION WITH EXPERIMENT.

In order to verify the accuracy of the numerical algorithm, a number of cases are simulated for which there are known analytical solutions. Figure 8 shows profiles at various times during the purely anisotropic etch of a three layer structure with an initially tapered, erodible mask. The taper angles of each layer are analytically related by the mask taper and etchrates [34] by:

$$\tan\beta_l = \frac{V_l}{V_u}\tan\alpha_u$$

where l signifies substrate layer and u the mask. Substrates that etch quickly form steep sidewalls, and those that etch more slowly form a more gradual taper. The simulated profiles agree to within one degree of the analytical solutions.

In a review paper, Mogab and Harshbarger [49] describe a number of plasma etching processes which are empirically classified as isotropic or anisotropic. Figure 9 clearly illustrates in a two step process a layer of polycrystaline silicon which has been anisotropically etched below a layer of isotropically overetched silicon dioxide. The simulation of these two processes, also shown in Figure 9, demonstrates in the two steps the two separate etching mechanisms. First, it uses the isotropic component to simulate the wet etching, say in HF, of the oxide layer. Then the shadowing and directional components are evident in the anisotropically etched polysilicon. Here, the simulation has used the two etching components in individual steps.

By identifying isotropic and anisotropic components from experimental information, a complete dry etching process can be simulated. Schwartz et al. [64] have published etchrates isolating the anisotropic and isotropic components, as well as scanning electron micrographs of reactively ion etched two layer structures. Here the combination of the two etchrate components effectively models the profile achieved in the reactive ion etching process, as shown in Figure 10. The silicon dioxide etches more anisotropically, while the silicon shows a more chemical, isotropic etch during the process. By adjusting the isotropic/anisotropic components,

other processing conditions, including the extreme cases of anisotropic and completely isotropic etching, may be simulated as well.

V. APPLICATIONS.

Two examples of dry etching processes are presented below to illustrate the usefulness of computer simulation in understanding experimental observation. The first case considers the anisotropic etching of a layer of isotropically deposited (by CVD, Chemical Vapour Deposition, technique) material on a non-uniform second layer. It is often observed (see Figure 11) that a residue remains near the bottom of a step under anisotropic etching conditions [21]. A simulation of this problem is shown in Figure 12 for a 0.7 μm step covered with a 0.7 μm layer. The step angle is varied 30^{o} to 90^{o} in the figures. In all cases the etchrate selectivity is 10:1, film:substrate. The thickness of the deposited layer vertically etches such that the maximum residue occurs at the concave corner of the step. Figure 13 shows the results of several simulations with no over etch. For more gradual steps the normalized residue, or overetch factor, converges to ($\sec\theta$ - 1) independent of the deposited thickness. For steep steps it approaches H/T, the step height divided by the deposited thickness. At intermediate values the over etch factor is reduced due to the curvature of the deposited profile.

The second example characterizes the enhancement of isotropic plasma etching by arsenic ion implantation. Figure 14 shows micrographs of etched polysilicon layers. The surface has been implanted with various arsenic doses. The etched profile depends on the amount of As implantation that the layer underwent. In Figure 15 a 0.1 μm layer of poly silicon has been implanted, then covered with an additional 0.5 μm of polysilicon. The composite is plasma etched in a barrel reactor resulting in the stepped profiles shown. The implanted layer in both cases, etches more quickly leading to various degrees of undercut. The profiles in Figure 14 were etched 15 minutes, at 15 Watts, 10 mTorr, 70^{o}C in $CF_4/5\%O_2$, and those in Figure 15 30 minutes, at 15 Watts, 10 mTorr, 70^{o} C in $CF_4/5\%O_2$. All implants were done at 30 KeV. Figure 16 plots the experimental stepped taper angle for the various implant doses. The larger the dose the more gradual is the step.

The use of stepped polysilicon layers in E^2IC [62,63] requires allowance for a certain amount of undercutting. Simulation can be used to study the amount of undercutting which must be tolerated. The process is modelled by layers of different etchrates depending on the implant dose. For example, Figure 17 shows the simulation of the time evolution of an implanted buried layer structure. It agrees quite closely with the time development in plasma etching, in Figure 18. Some second order effects become evident at the implanted/non-implanted interface, Figure 19, which the model does not include. The model does, however, clearly show the undercut necessary to produce the stepped profile.

Each of the above applications can be incorporated into the SAMPLE program via the TRIAL statement. There is a special additive rate function, SPECRT, which allows the user to specify his own special rates within a material layer. A piecewise linear profile specifies the nonuniform second layer and can be used when plasma etching follows evaporation and deposition.

REFERENCES

[1] H.Abe. "The Application of gas plasma to fabrication of MOSLSI." Sixth Conference on Solid State Devices, Tokyo 1974.

[2] D.J.Barber, F.C.Frank, M.Moss, J.W.Steeds, I.S.T.Tsong. "Prediction of ion-bombarded surface topographies using Frank's kinematic theory of crystal dissolution". *J.Mater.Sci. 8* (1973) 1030-1040.

[3] M.Baron & J.Zelez. "Vacuum systems for plasma etching, plasma deposition, and low pressure CVD". *Sol.St.Tech.*(December 1978) 61-65.

[4] J.F.Battey. "The effects of geometry on diffusion -controlled chemical reaction rates in a plasma". *J.of the ECS. 124.*(March 1977) 437.

[5] A.R.Bayly. "Secondary processes in the evolution of sputter topologies". *J.Mater.Sci. 7.* (1972) 404.

[6] R.L.Bersin. "Chemically selective, anisotropic plasma etching". *Sol.St.Tech.* (April 1978) 117.

[7] R.L.Bersin. "A survey of plasma etching processes". *Sol.St.Tech.* (May 1976) 31-36.

[8] L.D.Bollinger. "Ion milling for semiconductor production processes". *Sol.St.Tech.* (November 1977) 66-70.

[9] J.A.Bondur. "Dry process technology--reactive ion etching". *J.Vac.Sci.Tech., 13,* no.5, (1976) 1023.

[10] H.Boyd & M.Tang. "Applications of SiF_4 in plasma etching". *Sol.St.Tech.,22.* no. 4, (April 1979) 133-138.

[11] M.Cantagrel & M.Marchal. "Argon ion etching in a reactive gas". *J.of Mater.Sci. 8,* (1973) 1711-1716.

[12] M.Cantagrel. "Considerations on high resolution patterns engraved by ion etching". *IEEE Trans. on Electron Devices 22,* no. 7, (July 1975) 483-485.

[13] G.Carter, J.S.Colligon & M.J.Nobes. "Analytical model of sputter induced surface morphology". *Rad.Eff. 31,* (1977) 65-87.

[14] G.Carter, J.S.Colligon & M.J.Nobes. "The growth of topography during sputtering of amorphous solids--Part 4". *J.Mater.Sci. 8,* (1973) 1473-1481.

[15] C.Catana,J.S.Colligon,G.Carter. "The equilibrium topography of sputered amorphous solids--Part 3". *J.Mater.Sci. 7,* (1972) 467-471.

[16] L.T.Chadderton. "On a relationship between the geometry of cones on sputtered surfaces and the angular dependence of sputtered yields". *Rad.Eff, 33,* (1977) 129-32.

[17] S.Chung. "Determining a production plasma etch cycle". *Sol.St.Tech.* (April 1978) 114.

[18] H.A.Clark. "Plasma processing at moderate vacuums". *Sol.St.Tech.* (June 1976) 51-54.

[19] J.W.Coburn. "Sputtering in the surface analysis of solids". *J.Vac.Sci.Tech., 13,* no. 5, (1976) 1037-1043.

[20] J.W.Coburn & E.Kay. "Some chemical aspects of the fluorocarbon plasma etching of silicon and its compounds". *IBM J.Res.Dev. 23,* no. 1, (January 1979) 33.

[21] J.W.Coburn & H.F.Winters. "Plasma etching--a discussion of mechanisms". *J.Vac.Sci.Tech., 16,* no. 2 (March/April 1978) 391-401.

[22] J.W.Coburn & H.F.Winters. "Ion surface interactions in plasma etching". *J.of Appl. Phys., 48.*no. 8, (August 1977) 3532.

[23] P.D.Davidse. "RF sputter etching--a universal etch". *J.Elec. 116.*no. 1, (1969)

[24] J.P.Ducommun,M.Cantagrel,M.Marchal. "Development of a general surface contour by ion erosion. Theory and computer simulation". *J.Mater.Sci. 9,* (1974)725-736.

[25] J.P.Ducommun,M.Cantagrel,M.Moulin. "Evolution of well-defined surface contour submitted to ion bombardment: computer simulation and experimental investigation". *J.Mater.Sci., 10,* (1975) 52-62.

[26] D.L.Flamm. "Measurements and mechainisms of etchant production during the plasma oxidation of CF_4 and C_2F_6". *Sol.St.Tech., 22,* no. 4 (April 1979) 109-116.

[27] P.G.Gloersen. "Ion beam etching". *J.Vac.Sci.Tech., 12,* no. 1 (1975) 28-34.

[28] W.R.Harshbarger & R.A.Porter. "A study of optical emission from a RF plasm during etching". Bell Lab. 1976.

[29] R.Heinecke. "Plasma reactor design for selective etching of SiO_2 on Si". *Sol.St.Elec., 19,* (1976) 1039-1040.

[30] Hollahan & Bell. Semiconductor device fabrication. from *Applications in Plasma Chemistry,* cpright 1974.

[31] W.R.Hudson. "Ion beam texturing". *J.Vac.Sci.Tech. 14,* no. 1 (1977) 286-289.

[32] T.Ishitani, M.Kato, R.Shimizu. Comments on "The equilibrium topography of sputtered amorphous solids" *J.Mater.Sci. 9,* (1974) 505-508.

[33] R.E.Jewett, P.I.Hagouel, A.R.Neureuther, & T.Van Duzer. "Line-profile resist development simulation techniques". *Poly.Eng.Sci. 14, no. 6, (June 1977) 381-384.*

[34] K.Jinno & S.Inomata. "Study of plasma etching reactions and photoresist performance in CF_4-O_2 plasmas". Translation provided courtesy of the International Plasma Corporation, Hayward, CA.

[35] S.H.Keller, R.G.Simmons. "Sputtering process model of deposition rate". *IBM j.Res.Dev. 23,* 1, (January 1979) 24.

[36] H.Kinoshita. "Anisotropic etching of Si by gas plasma". *Jap.J. of Appl.Phys. 16,* no. 2, (1977) 381-382.

[37] H.Komiya & H.Toyoda. "Analysis of line width and undercutting during plasma etching of Si_3N_4". *Jap. J. of Appl.Phys.* Seventh conference on Solid State Devices. (September 1975)

[38] R.Kumar, C.Ladas & G.Hudson. "Characterization of plasma etching for semiconductor applications". *Sol.St.Tech.*
(October 1976) 54-59.

[39] R.LeClaire. "Advances in planar plasma etching equipment". *Sol.St.Tech. 22,* no. 4, (April 1979) 139-142.

[40] H.W.Lehmann, Krausbauer, & R.Widmer. "Redeposition --a serious problem". *J.Vac.Sci.Tech. 14,* no. 1 (1977) 281-284.

[41] H.W.Lehman & R. Widmer. "Fabrication of deep square wave structures with micron dimensions by reactive sputter etching". *Appl.Phys.Letters 32,* no. 3 (1963)

[42] H.W.Lehmann & R.Widmer. "Profile control by reactive sputter etching". *J.Vac.Sci.Tech. 15,* no. 2 (March/April 1978)

[43] L.Mader & J.Joepfner. "Ion beam etching of SiO_2 on Si". *J.ECS 123,* no. 12 (December 1976) 1893-1898.

[44] R.L.Maddox & H.L.Parker. "Applications of reactive plasma practical microelectronic processing systems". *Sol.St.Tech.,* (April 1978) 107.

[45] S.Matsuo. "Preferential SiO_2 etching on Si substrate by reactive sputter etching". *Jap. J. of Appl.Phys. 16,* no. 1, (1977) 175-176.

[46] S.Matsuo. "Etching characteristics of various materials by plasma reactive sputter etching". *Jap. J. of Appl.Phys. 17,* no. 1, (1978) 235-236.

[47] C.M.Meliar-Smith. "Ion etching for pattern delineation". *J.Vac.Sci.Tech. 8,* no. 5 (1976) 1008-1021.

[48] C.J.Mogab. "The loading effect in plasma etching". *J.ECS* (August 1977) 1262-1268.

[49] C.J.Mogab & W.R.Harshbarger. "Plasma processes set to etch finer lines with less undercutting". *Electronics 115,* (August 31, 1978) 117.

[50] S.N.Nandgaonkar. "Design of a simulator program (SAMPLE) for IC fabrication". M.S.Thesis, Electronics Research Laboratory, Univ. of California, Berkeley (1978)

[51] A.R.Neureuther, R.E.Jewett, P.I.Hagouel, & T.Van Duzer. "Surface etching simulation and applications in IC processing". Proc. Lodak Microelectronics seminar "Interface '76", Monterey, CA (October 3-5, 1976) 81-91.

[52] A.R.Neureuther, M.M.O'Toole, W.G.Oldham, & S.N.Nandgaonkar. "Use of simulation to optimize projection printing profiles". 153rd meeting of the ECS, Seattle, (May 21-26, 1978).

[53] M.M.O'Toole. "Simulation of optically formed image profiles in positive resist". Ph.D. Thesis. Electronics Research Laboratory, University of California, Berkeley. (June 1979)

[54] W.G.Oldham, S.N.Nandgaonkar, A.R.Neureuther, & M.M.O'Toole. "A General simulator for VLSI lithography and etching processes, Part I--Application to projection lithography". *Trans. on Electron Devices 26*, no. 4 (April 1979) 717-722.

[55] H.Oni & H.Tango. "A new technology for tapered windows in insulating films". *J.ECS 12*, (March 1979) 504-506.

[56] P.D.Parry & A.F.Rodde. "Anisotropic plasma etching of semiconductor materials". *Sol.St.Tech. 22*, no.4, (April 1979) 125-132.

[57] R.G.Poulsen. "Plasma etching in IC manufacture". *J.Vac.Sci.Tech. 14*, no.1 (1977) 266.

[58] R.G.Poulsen & M.Brochu. "Importance of temperature and temperature control in plasma etching". Etching for pattern definition, ECS symposium series. (1976)

[59] A.R.Reinberg. "Plasma etching in semiconductor manufacture". Etching for pattern definition, ECS symposium series. (1976)

[60] D.D.Robertson. "Advances in ion beam milling". *Sol.St.Tech.*, (December 1978) 57.

[61] L.T.Romankiw. "Pattern generation in metal films using wet chemical techniques". Etching for pattern definition, ECS symposium series. (1976)

[62] T.Sakai et al. "Stepped electrode transistor". Proc. Eighth conf. (1976 int.) on Solid-State Devices, Tokyo, Japan, 196-197.

[63] T.Sakai et al. "Elevated Electrode Integrated Circuits". *IEEE Trans. on Electron Devices 26*, no.4 (April 1979) 379-384.

[64] G.C.Schwartz, L.B.Rothman & T.J.Schopen. "Competing mechanisms in reactive ion etching in a CF_4 plasma". *J.ECS 12*, (March 1979) 464-469.

[65] G.C.Schwartz,L.B.Zielinski & T.J.Schopen. "Reactive ion etching". Etching for pattern definition, ECS symposium series. (1976)

[66] P.Sigmund. "A mechanism of surface micro-roughening by ion bombardment". *J.Mater.Sci. 8*, (1973) 1545-1553.

[67] H.I.Smith. "Ion beam etching". Etching for pattern definition, ECS symposium series. (1976)

[68] S.Somekh. "Introduction to ion and plasma etching". *J.Vac.Sci.Tech. 13*, no. 5, (1976) 1003-1007.

[69] S.Somekh & H.C.Casey,Jr. "Dry processing of high resolution and high aspect ratio structures in GaAs-$Al_xGa_{1-x}As$ for integrated optics". *Appl.Optics. 16*, no. 1 (January 1977) 126-136.

[70] K.Suzuki et al. "Microwave plasma etching". *Jap. J. of Appl.Phys. 16*, no. 11, (November 1977) 1979-1984.

[71] I.S.T.Tsong & D.J.Barber. "Development of surface topography on Silica glass due to ion bombardment". *J.Mater.Sci. 7*, (1972) 687-693.

[72] K.Ukai & K.Hanazana. "Analysis of the imaging accuracy in reactive ion etching". *J.Vac.Sci.Tech. 15*, no. 2, (1978) 338.

[73] N.Vishwanathan. "Simulation of plasma-etched lithographic structures." *J.Vac.Sci.Tech. 16*, no. 2 (March/April 1979)

[74] M.J.Wilcomb. "Conical topography formed on ion etched crystalline surfaces". *J.Appl.Phys. 46*, no. 11, (1975) 5053.

[75] I.H.Wilson. "The topography of sputtered semiconductors". *Rad.Eff. 18*, (1973) 95-103.

[76] H.F.Winters. *Physical sputtering: A discussion of experiment and theory.* .

[77] M.J.Witcomb. "Dissolution applied to the prediction of apex angles of conical ion-bombardment structures". *J.Mater.Sci. 10*, (1975) 669-81.

[78] Zarowin. "A Theory of plasma chemical transport --comparison with experiment for the etching and deposition of Au in a Cl_2 plasma".

APPENDIX A

KEYWORD DESCRIPTIONS

Notes on symbols and conventions:

UPPER CASE BOLD indicates keywords and commands.
lower case italics indicates numerical values.
UPPER CASE ROMAN indicates common block variable names.
[ ] bracketed variables or words indicates optional.
{ } braced variables or words indicates alternatives.
( ) parenthesized words specify units of the numerical values.

Inputting a profile without running the develop machine.

MODEL CONTOURS {**LINE** } *dimension* (in microns)
{**SPACE**} *dimension* (in microns)
{**EDGE** }

LINE inputs line of width *dimension* centered in WINDOW.

SPACE inputs a space of width *dimension* centered in WINDOW.

EDGE inputs a falling edge centered in WINDOW

--or--

MODEL CONTOURS $(x,z)_1, (x,z)_2, \ldots (x,z)_p$ (in microns).

The coordinates $(x,z)_i$ are the turning points in a piecewise linear profile.

Associated common block variables in /PROF /

IPVAR=1 signifies LINE
IPVAR=2 signifies SPACE
IPVAR=3 signifies EDGE
DIMEN=*dimension*
PXZ(i)=$(x,z)_i$
IPLAST=*p*. (p<12)

Inputting horizontal dimensions.

WINDOW OUTPUT x_1 x_2 (in microns)

x_1 is the horizontal width of the output window.

x_2 is the distance from the left side of the window to the edge of the mask. It is not applicable to the etching routines.

Associated common block variables in /ETHWND/

HORWIN=x_1

Inputting vertical dimensions as layer thicknesses.

{NITRIDE}
LAYER *layer#n* {**OXIDE**} *thickness* (in microns)
{**RESIST**}
{**SPECIAL**}

layer#n places the layer, *#n* = 0 means substrate, 1 the next layer and the greatest number is the topmost layer.

NITRIDE, OXIDE, RESIST, SPECIAL also specify the layer, especially concerning default values and material parameters.

thickness is the layer thickness in microns.

Associated common block variable in /THKNES/

THICK(NMLYRS-*#n*) = *thickness*

Inputting etching parameters.

Plasma Etching:

MODEL *layer#n* ETCH R_1 [R_2] (in microns/min)
[SOURCE ETCH θ (in degrees)]

layer#n indicates the layer to which the etching parameters refer.

R_1 is the isotropic, nondirectional etchrate in microns/minute. If only isotropic etching is to be preformed this is the only number needed.

R_2 is the illuminated, directional etchrate in microns/minute.

θ is the angle in degrees of the incident radiation flux when directional etching is being used. 0^0 means direct incidence and positive angles from the left.

Associated common block variables in /ISOETH/ & /ILETCH/.

RISOTR(NMLYRS-#n) = R_1
RTISO(NMLYRS-#n) = R_1
RTNORM(NMLYRS-#n) = R_2
DANGLE = θ

Ion Milling and Sputtering:

MODEL *layer#n* IONETCH S_0(#n) [ρ(#n) A(#n) B(#n) C(#n)]
SOURCE IONETCH θ (in degrees) ϕ (in ions/cm^2)

S_0 is the sputter etch rate at normal incidence in 1/seconds for layer *n*.

ρ is the density of layer *n* in ions/cm^2.

θ is the angle of flux incidence in degrees.

ϕ is the flux density of the incoming ion beam in ions/cm^2.

A(#n), B(#n), and C(#n) are the analytic coefficients that model the angular dependent sputtering yield as a cosine power series.

Associated common block variables in /SPUTYD/:

ASPUT(NMLYRS-#n) = A(#n)
BSPUT(NMLYRS-#n) = B(#n)
CSPUT(NMLYRS-#n) = C(#n)
DENS(NMLYRS-#n) = ρ(#n)
SPTYD0(NMLYRS-#n) = S_0(#n)
PHI = ϕ
DANGLE = θ

Inputting the etching times.

TIME ETCH t_1 [TO t_2 IN *n*]

t_1 is the first output time or optionally the single output time.

t_2 is specified when more than one output time is desired. It gives the final output time of a range.

n is the number of outputs. Each output is equally spaced in time within the range t_1 to t_2.

Associated common block variables in /ETCHTM/.

EHTM1 = t_1
EHTM2 = t_2
NMEHTM = n

Instructions for printing and plotting.

PLOT [DP]

PRINT {DEBUG}
{CONTOURS}

PLOT plots the output contours on the lineprinter.

PLOT DP punches cards with the contours coordinates for a digital plotter.

PRINT DEBUG prints diagnostics concerning string point model.

PRINT CONTOURS prints the coordinates of the string points numerically.

Associated common block variables.

INDVAR(2) = 0(off),1(on)	**PLOT DP**
INDVAR(5) = 0(off),1(on)	**PRINT DEBUG**
INDVAR(6) = 0(off),1(on)	**PRINT CONTOURS**
INDVAR(7) = 0(off),1(on)	**PLOT**

Accuracy.

ACCURACY *k*

k is an integer between 0 and 5, where 5 demands the most accuracy and 0 the least. 2 is the default value.

Associated common block variable in /INDCAT/.

INDVAR(3) = *k*

Running the etch routines.

{DESCUM}
RUN {ETCH}
{IONETCH}

DESCUM simulates descumming the resist layer isotropically.

ETCH simulates plasma etching.

IONETCH simulates ion milling and sputtering.

Associated common block variable in /INDCAT/.

INDVAR(4) = 0 no **RUN** command.
= 1 **RUN ETCH** with one etchrate specified.
= 2 **RUN ETCH** with two etchrates specified.
= 3 **RUN DESCUM**
= 4 **RUN IONETCH**
= 5, 6 using **TRIAL** statement.

DEFAULTS AND TYPICAL VALUES

The consistency of the default values arises from the assumptions that all parameters indexed by 1 represent RESIST and it's defaults, 2 SPECIAL (polycrystaline silicon), 3 NITRIDE (silicon nitride), 4 OXIDE (silicon dioxide), and 5 SUBSTRATE (<100> silicon).

Plasma etching defaults				
Variable	thick(n)	risotr(n)	rtiso(n)	rtnorm(n)
Units	microns	microns/minute	microns/minute	microns/minute
Material	thickness	isotropic	non-directional rate	directional rate
1 RESIST	0.800	0.0060	0.0005	0.0010
2 SPECIAL	0.600	0.3000	0.0300	0.0360
3 NITRIDE	0.300	0.0300	0.0120	0.0430
4 OXIDE	0.080	0.0125	0.0060	0.0390
5 SUBSTRATE	0.200*	0.2040	0.0300	0.0360

*This is not the actual thickness of the substrate, but the amount that will appear in the output plot.

General defaults			
Variable	Description	Value	Units
indvar(1)	type of profile	2	...
indvar(2)	card punch	0	...
indvar(3)	accuracy	2	...
indvar(4)	type of etch	2	...
indvar(5)	diagnostics	0	...
indvar(6)	print coordinates	0	...
indvar(7)	line print profiles	1	...
ipvar	profile=line	1	...
dimen	linewidth	1.0	microns
horwin	window size	4.0	microns
nmlyrs	number of layers	5	...
dangle	angle of incidence	0.0	degrees
phi	ion flux	.32	milliAmp/cm^2
ehtm1	initial etch time	400.	seconds
ehtm2	final etch time	1000.	seconds
nmehtm	number of profiles	4	...

Typical values in ion milling							
Material	S_o	density	A	B	C	max angle	max:norm
AZ1350	2000.	3.00	1.3513	2.7048	-3.0561	40	1.57
poly	4272.	4.98	7.8776	-4.8938	-1.9838	52	2.71
NITRIDE	817.	1.48	7.8776	-4.8938	-1.9838	52	2.71
OXIDE	959.	2.66	7.8776	-4.8938	-1.9838	52	2.71
SILICON	4272.	4.99	3.2696	13.1059	-15.3755	60	3.95
Gold	5310	5.89	8.2	-8.8	1.6	0	1.00
GaAs	1460	1.54	1.1551	3.2936	-3.4487	40	1.63
Aluminum	33500	6.02	3.4142	1.7974	-4.2116	45	2.26
Titanium	595.	5.66	-3.8085	12.0708	-1.9838	35	1.71

CONTROL CARD SUMMARY

control card	keyword	parameter
ACCURACY	integer	
-		
LAYER layer#	NITRIDE OXIDE RESIST SPECIAL	thickness
-		
MODEL layer#	DESCUM ETCH IONETCH	rate rates rates [density analytics]
-		
PLOT	[DP]	
-		
PRINT	DEBUG CONTOURS	
-		
RUN	DESCUM ETCH IONETCH	
-		
SOURCE	ETCH IONETCH	angle (degrees) angle fluxdensity
-		
TIME	ETCH	t_1 [TO t_2 n]
-		
TITLE		
-		
WINDOW	OUTPUT	width

APPENDIX B

COMMON BLOCK DESCRIPTION

Common blocks that are
common to the photoresist
developing routines.

/DEVFLG/

Develop flags are common to the Controller and to Subroutines CHKR and DELOOP.

IDEVFL(5)-- a one dimensional array containing the flags for machine DELOOP and CHK signifies [yes], 0 [no].

IDEVFL(1) {=INDVAR(5)} prints the number of string points and other diagnostics from CHKR and DELOOP. {cf keyword PRINT DEBUG; consistency with INDVAR(5) is insured in controller}

/DVELP1/

Development block 1 is internal to Subroutines RIETCH, CHKR, DELOOP, STPRFL, ADJUST, RIEADV, SHADOW, ETHMSG, PLTDGT, PRTNUM, PLTLPR, and funs DIST and PROJ.

XZ(450)-- complex array containing the x and z positions of the 450 possible string-points.

XMAX-- the real maximum value of x.

ZMAX-- the real maximum value of z; the summation of the layer thicknesses.

NPTS-- the current number of string-points.

CXZL-- the normalized left endpoint direction of etching.

CXZR-- the normalized right endpoint direction of etching.

NADCHK-- the number of advances (calls on Subroutine RIEADV) between checks (cal Subroutine CHKR).

NCKOUT-- the number of checks between outputs, {thus the number of advances bet outputs is NADCHK*NCKOUT}.

/DVELP2/

Development block 2 is internal to Subroutines RIETCH, CHKR, DELOOP and RIEADV.

TADV-- the current time increment between advances (in RIEADV)

TCHK-- the current time increment between checks.

TTOT-- the total current etching time during the execution of RIETCH.

IFLAG-- flag set in RIEADV that indicates some segments are long or too short. CHKR is then called from RIETCH.

SMAXX-- the maximum x string segment length allowed by CHKR.

SMINX-- the minimum x string segment length allowed by CHKR.

SMAXZ-- the maximum z string segment length allowed by CHKR.

/IO1 /

Input/output block 1 is common to all subroutines and Controller. The block is decided in the top level controller for handling input/output in a uniform way. It contains the symbollic names for logical input/output unit numbers.

IPRINT-- the correct character to access the printer with the FORTRAN statement "WRITE(IPRINT,###)".

IPUNCH-- the correct character to access the card puncher with the FORTRAN statement "WRITE(IPUNCH,###)".

/THKNES/

MNLYRS-- the maximum number of layers allowed in the problem. The first layer is the resist layer; the last is the substrate. Four intermediate layers are allowed.

NMLYRS-- the number of layers in the current problem.

THICK(6)-- a one dimensional array containing the thicknesses of the various layers in microns characterized by etchrates RTNORM, RTISO, RISOTR, and SPTYD0. THICK(NMLYRS) is the amount of the substrate that that is shown in the output. {cf keyword LAYER}

Common blocks initialized
in the etching simulation

/ETCHTM/

Etch times is common to the Controller and Subroutines RIETCH, ETHMSG, PLTDGT, PRTNUM, and PLTLPR.

MXNEHT-- maximum number of timed etched outputs allowed in a single problem. Currently, it is 20.

NMEHTM-- number of output profiles specified for a problem. {cf keyword TIME ETCH}

NCOEHT-- index of the current output profile.

EHTM1-- the etching time in seconds of the first output profile. {cf keyword TIME ETCH}

EHTM2-- the etching time in seconds of the last output profile. {cf keyword TIME ETCH}

EHTM-- the etching time in seconds of the current output profile.

EHTMST-- the time step between output profiles.

/ETHPAR/

Etching parameters is common to Subroutines RIETCH, PLTLPR, and STPRFL.

NSTPTS-- number of points in the initial profile created by STPRFL; the number increases with accuracy.

DELTXE-- the horizontal spacing of points in the initial profile created by STPRFL.

DELTZE-- the vertical spacing of points in the initial profile created by STPRFL.

/ETHWND/

Etch window is common to the Controller and to the RIETCH, STPRFL, COMPAT, PLTLPR, PLTDGT, and PRTNUM Subroutines.

HORWIN-- the x (horizontal) window width in microns; it is set by the Controller. {cf. keyword WINDOW OUTPUT}

VERWIN-- the z (vertical) window length in microns; it is the summation of the layer thicknesses for etching routines and the photoresist thickness in descumming.

/ILETCH/

Illuminated etching coefficients is common to the Controller, Functions RIERT, RISORT, and Subroutines RIETCH and ETHMSG.

RTNORM(6)-- the one dimensional array specifying the directional etchrates at normal incidence for each layer. {cf. keyword MODEL layer# ETCH}

RTISO(6)-- the one dimensional array specifying the background, isotropic etchrates for each layer. {cf. keyword MODEL layer# ETCH}

DANGLE-- angle in degrees of the incident radiation flux. {cf. keyword MODEL SOURCE ETCH theta}

/INDCAT/

Indicator variables are common to the Controller and Subroutines RIETCH, RIEADV, PLTLPR, AIMPLT, and STEP.

INDVAR(6)-- The one dimensional array specifying the different options for the etching routines.

INDVAR(1)--type of profile input.

- 0 stop with the development of the resist.
- 1 continue etching from the developed resist profile.
- 2 create an initial profile by specifying coordinates for a piecewise linear profile. {cf. keyword MODEL CONTOURS}
- 3 read the string points from a tape, cards or file, and continue etching. {cf keyword LOAD}

INDVAR(2)--cards for the etched profile. {cf. keyword PLOT DP}

- 0 no cards punched.
- 1 cards punched in the format /4 corners of output graph/ number of outputs/number of points in output/coordinates of each string point/

INDVAR(3)--accuracy {cf keyword ACCURACY #}

- 0-5 0 being the least accurate, and 5 being the most accurate. INDVAR(3) controls number of initial points, spacing between points, and the number of advances per output.

INDVAR(4)--type of etching. {cf keywords such as ETCH, IONETCH, DESCUM or TRIAL}

- 0 no etching or descum after resist development.
- 1 isotropic or wet etching.
- 2 reactive ion or plasma assisted etching.
- 3 descum of the photoresist.
- 4 ion milling or sputter etching.
- 5 special etching feature with regions of different etchrate.
- 6 etching over a non-uniform second layer.

INDVAR(5)--diagnostics as points are added and deleted. [=IDEVFL(1)] {cf. keyword PRINT DEBUG}

- 0 no diagnostics.
- 1 diagnostics from CHKR.

INDVAR(6)--coordinates of string point contours are printed numerically. {cf. keyword PRINT CONTOURS}

- 0 off.

1 coordinates printed numerically.

INDVAR(7)-- line printer plots the contours with coordinates marked as alphabetics. {cf. keyword PLOT}

0 off.

1 line printed plot.

/ISOETH/

Isotropic etching components are common to the Controller, Subroutines ETHMSG and AIMPLT, and Function SPECRT.

RISOTR(6)-- a one dimensional array specifying the isotropic (non-directional) etchrate for each layer. {cf. keyword MODEL layer# ETCH}

/PROF /

Profile information is common to the Controller and Subroutines STPRFL, ETHMSG, and STEP.

PXZ(12)-- a complex array of the twelve possible (x,z) coordinates used in creating the initial, piecewise linear profile. {cf. keyword MODEL CONTOURS}

IPLAST-- the number of coordinate pairs which set the initial profile. {cf. keyword MODEL CONTOURS}

IPVAR-- the indicator variable for default and preset profiles. {cf. keyword MODEL CONTOURS}

0 All profile turning points must be specified.

1 A line of width DIMEN centered in CPWIND

2 A space of width DIMEN centered in CPWIND

3 A step with the falling edge centered in CPWIND

4 A specially saved profile.

DIMEN-- The dimension of the feature indicated by IPVAR. {cf. keyword MODEL CONTOURS}

/SHADE /

Shade, which contains information about the direction of the radiation flux, is internal to Subroutines RIETCH, RIEADV, SHADOW, ADJUST, ETHMSG and Functions DIST and PROJ.

SLOPE-- the slope of a line parallel to the radiation flux.

FACTOR-- -/(SLOPE**2 + 1)

ANGLE-- the angle of incidence in radians of radiation flux.

MSHADE(450)-- a one dimensional array of flags specifying the exposure of a string-point; 1 means in shadow, 0 exposed.

/SPUTYD/

SPUTYD contains information about ion milling and sputtering and is common to the Controller , Subroutines RIETCH, ETHMSG, and function RIMRATE.

ASPUT(6)-- a one dimensional array specifying the coefficient in the sputtering yield analytic, $S(\theta) = A\cos\theta + B\cos^2\theta + C\cos^4\theta$, for each layer. {cf. keyword MODEL layer# IONETCH}

BSPUT(6)-- a one dimensional array specifying the coefficient in the sputtering yield analytic, $S(\theta) = A\cos\theta + B\cos^2\theta + C\cos^4\theta$, for each layer. {cf. keyword MODEL layer# IONETCH}

CSPUT(6)-- a one dimensional array specifying the coefficient in the sputtering yield analytic, $S(\theta) = A\cos\theta + B\cos^2\theta + C\cos^4\theta$, for each layer. {cf. keyword MODEL layer# IONETCH}

SPTYD0-- a one dimensional array specifying the sputtering yield at normal incidence, 0^o, for each layer in 1/seconds. {cf. keyword MODEL layer# IONETCH}

DENS(6)-- a one dimensional array specifying the density of each layer material in atoms/cm^2. {cf. keyword MODEL layer# IONETCH}

PHI-- the incident ion flux density in milliamperes/cm^2. {cf. keyword MODEL SOURCE IONETCH theta phi}

Common blocks inserted
for special purposes and
TRIAL runs

/IMPLNT/

Implant information is common to TRIAL, Subroutines AIMPLT, ETHMSG, and Function SPECRT.

QCM2-- the implant dose in fluence/cm**2.

DOSKEV-- the implant energy in KeV.

RANGE-- the average depth of penetration of implanted ions.

STNDEV-- the standard deviation in the implantation depth.

DNSCM3-- the density in ions/cm**3 of ions in the implanted material.

/SPCIAL/

Special information block 1 is common to TRIAL, Subroutines ETHMSG and AIMPLT, and Function SPECRT.

IFLSPC-- flag identifying the position of the implanted layer (surface = 1 or buried = 2)

RTSPEC(6)-- a one dimensional array specifying the etchrates within the regions defined by RLAYER(6).

/SPC2 /

Special information block 2 is common to TRIAL, Subroutines ETHMSG and AIMPLT, and Function SPECRT.

RLAYER(6)-- The thicknesses in microns of regions (within material layers) of various etchrates (RTSPEC(6)).

NLAYER-- the number of regions of differing etchrates.

BURLYR-- the thickness in microns of the buried layer with a different etchrate.

/NUNFRM/

Step information is common to TRIAL, Subroutines ETHMSG and STEP, and all rate functions.

STPSLP-- slope of the piecewise linear non-uniform second layer.

XINCPT-- x-intercept of the non-uniform second layer.

GAMMA-- angle the non-uniform layer makes with the horizontal.

LSTEP-- flag specifying a non-uniform layer in rate functions.

PI-- 3.1415926...

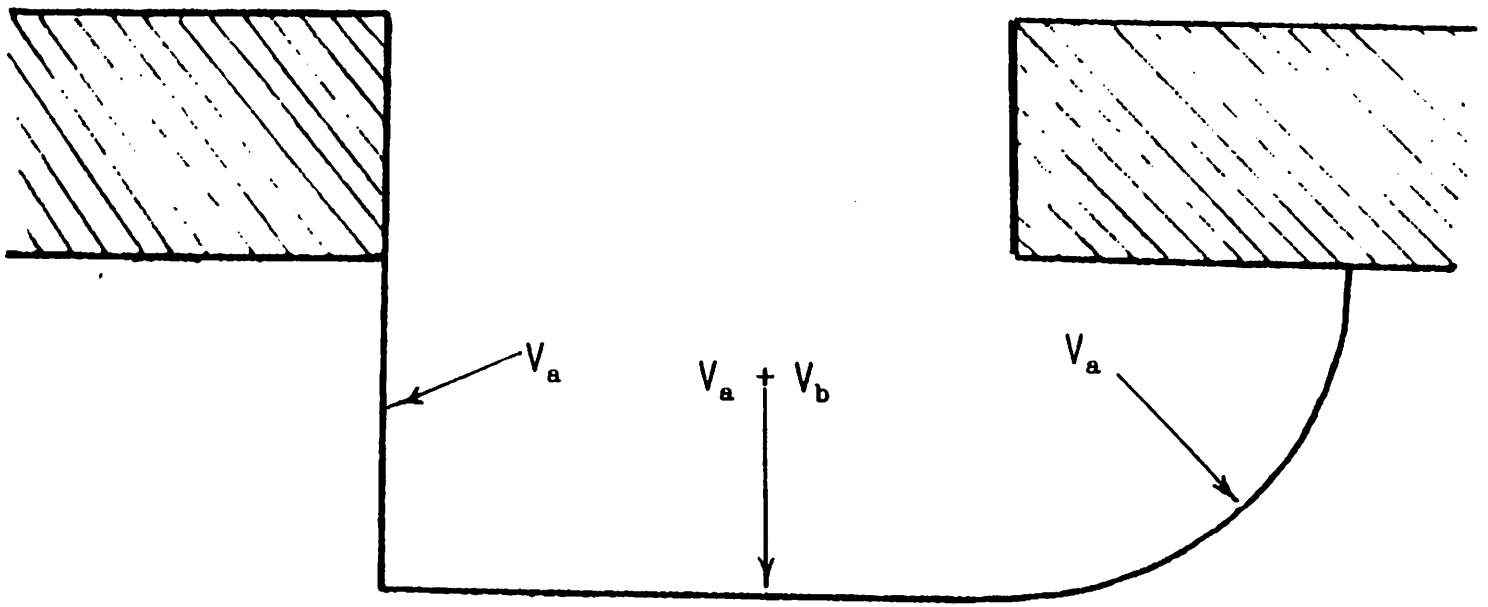

FIGURE 1 : ISOTROPIC AND DIRECTIONAL ETCHRATES AS THEY APPLY TO A MASKED SURFACE, A). ISOTROPIC ON SIDE B). DIRECTIONAL AND ISOTROPIC ON EXPOSED SURFACE, AND C). ISOTROPIC ON SHADOWED SURFACE.

FIGURE 2.

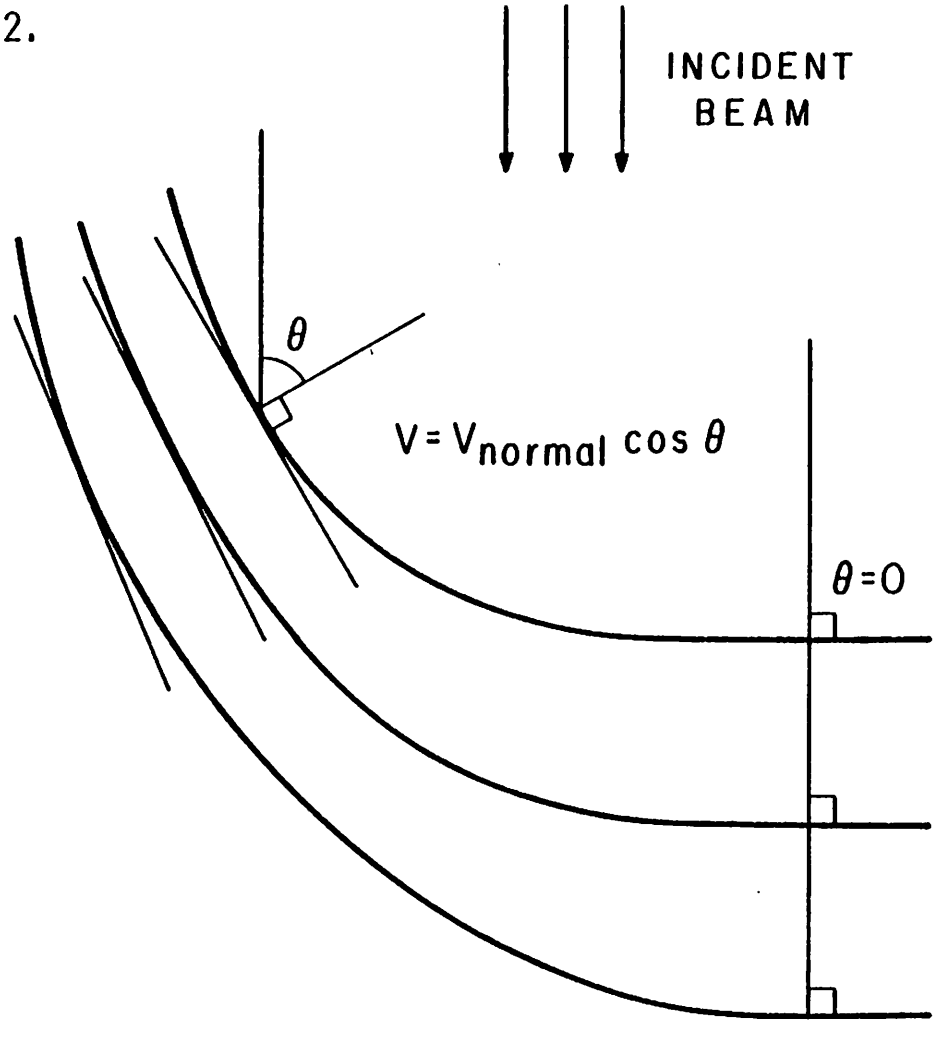

LOCAL ANGULAR DEPENDENCE

FIGURE 3.

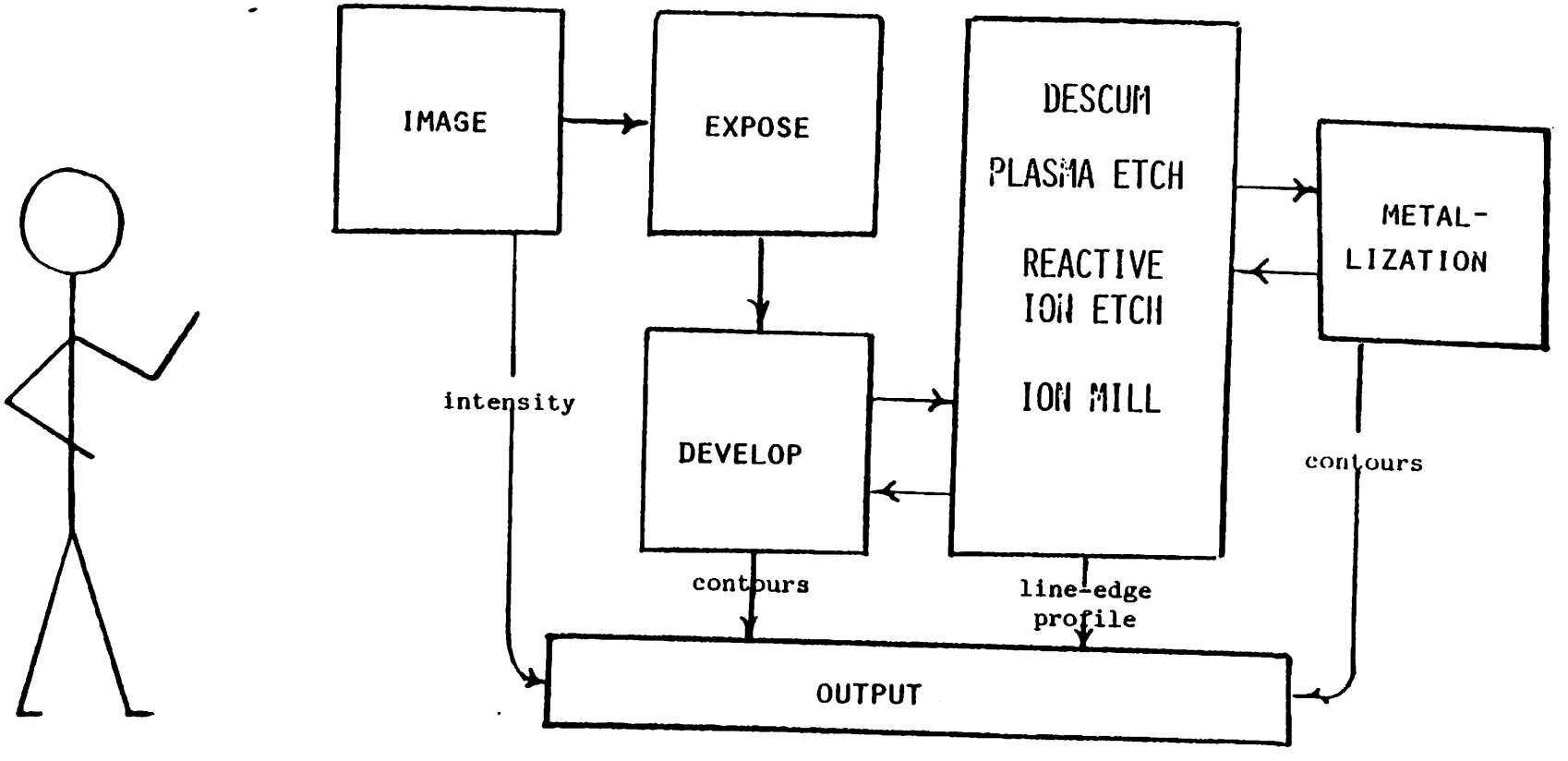

SIMULATION AND MODELLING OF PROFILES IN LITHOGRAPHY AND ETCHING

--SIMULATOR STRUCTURE

FIGURE 4: ISOTROPIC AND ANISOTROPIC ADVANCES OF POINTS ALONG LINE-EDGE PROFILE.

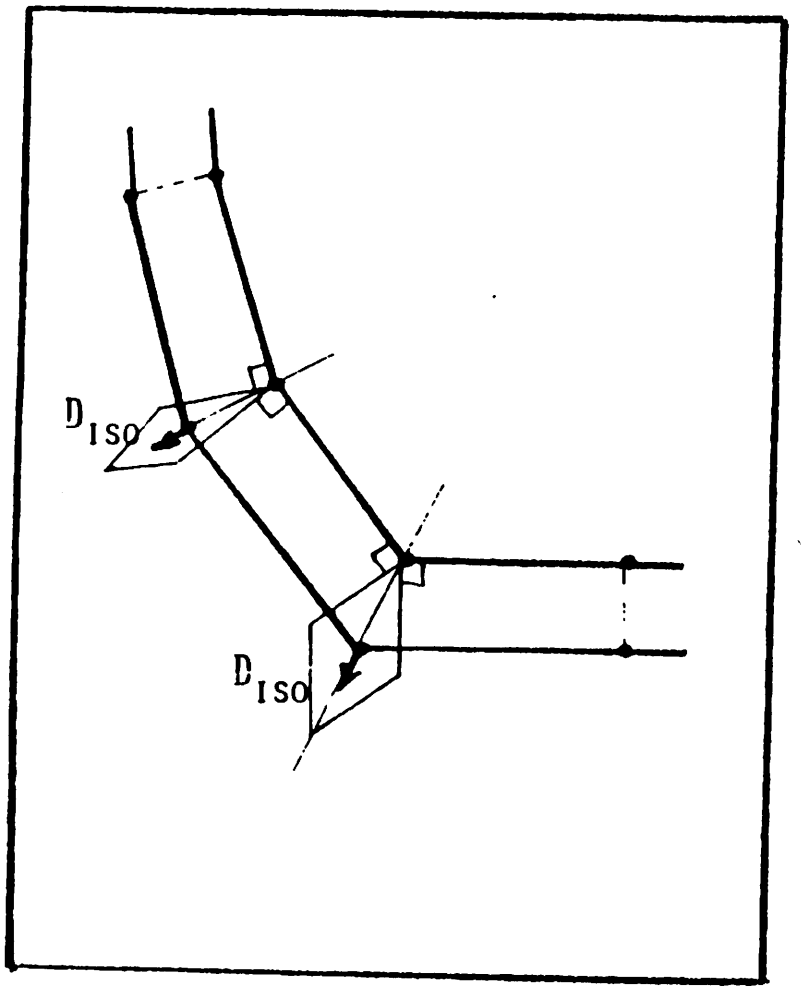

ISOTROPIC

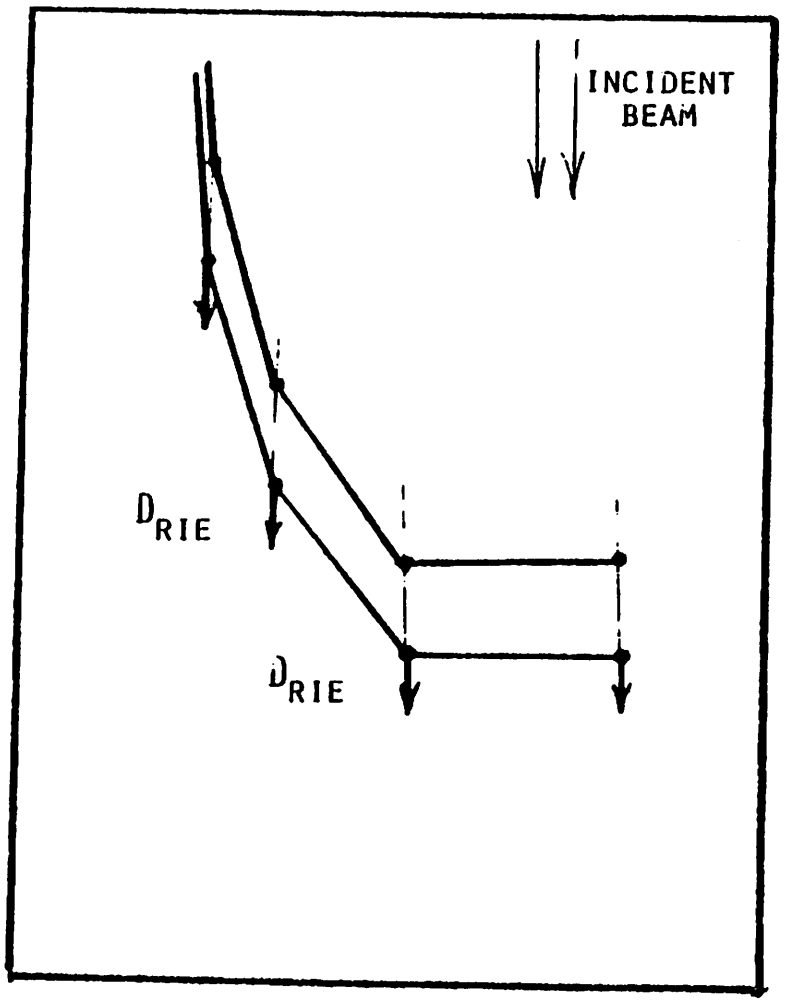

ANISOTROPIC

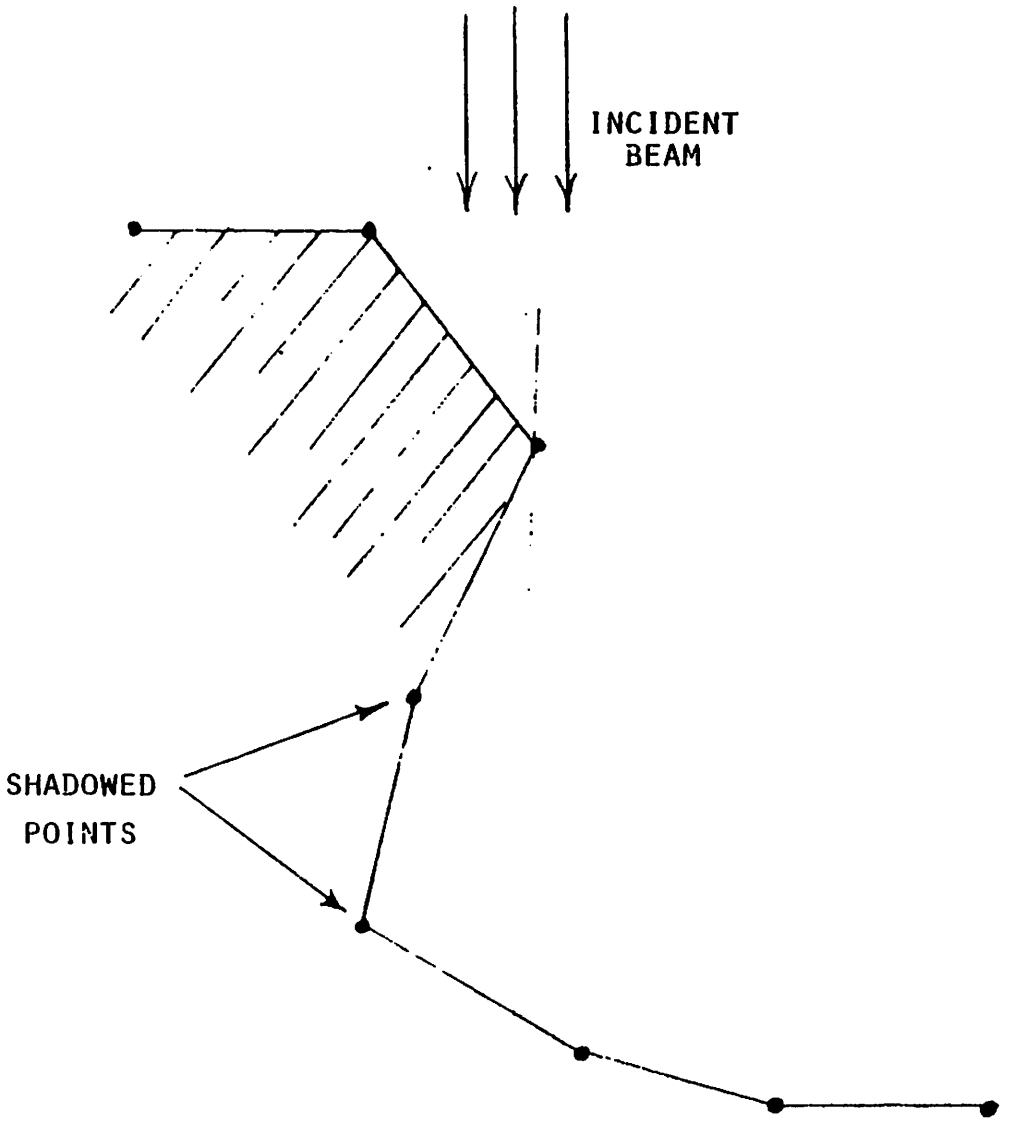

FIGURE 5: SHADOWED POINTS ALONG THE STRING.

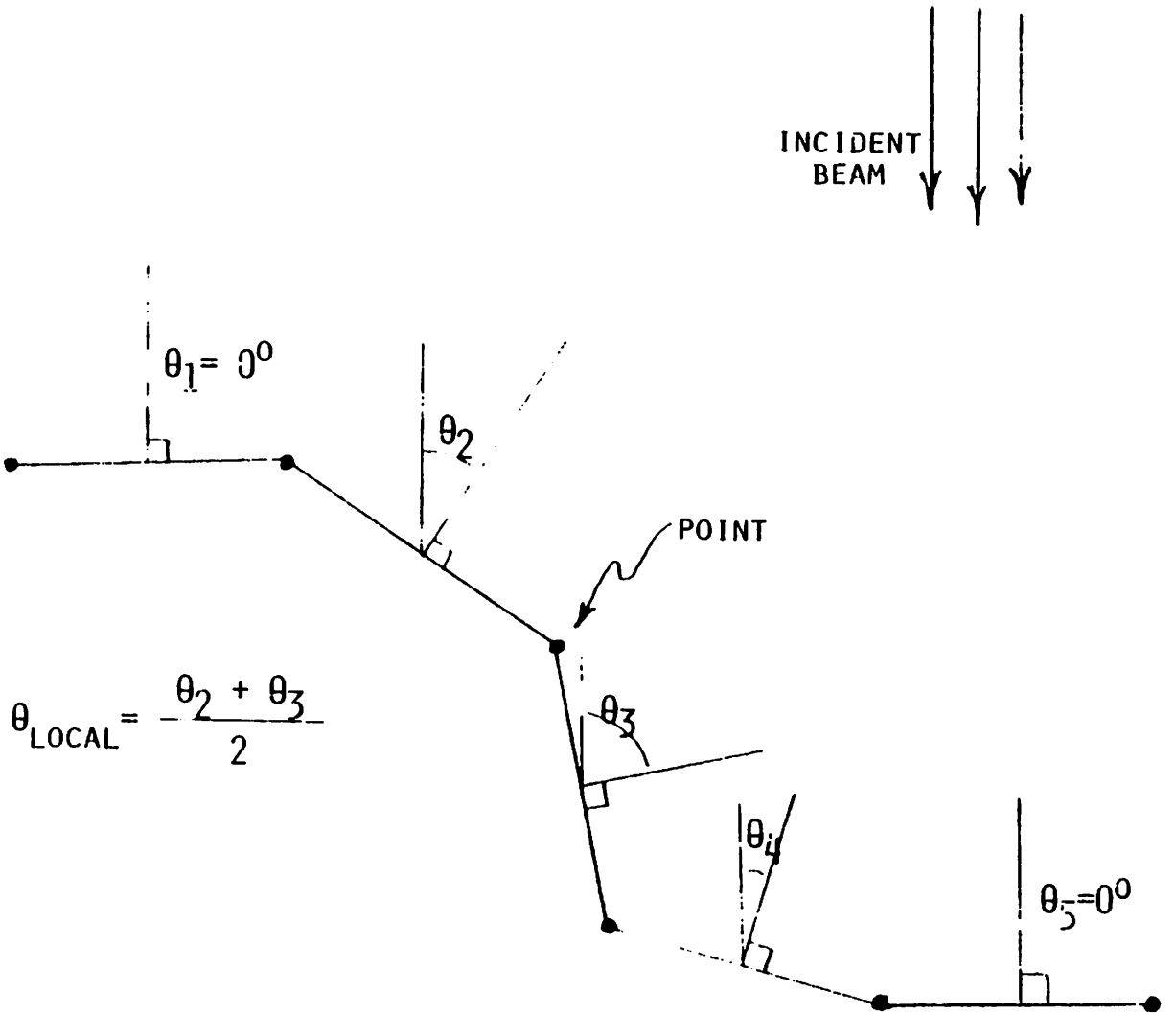

FIGURE 6: EXTRACTION OF LOCAL ANGULAR ORIENTATION FROM STRING IN ION MILLING MODELLING.

FIGURE 7.

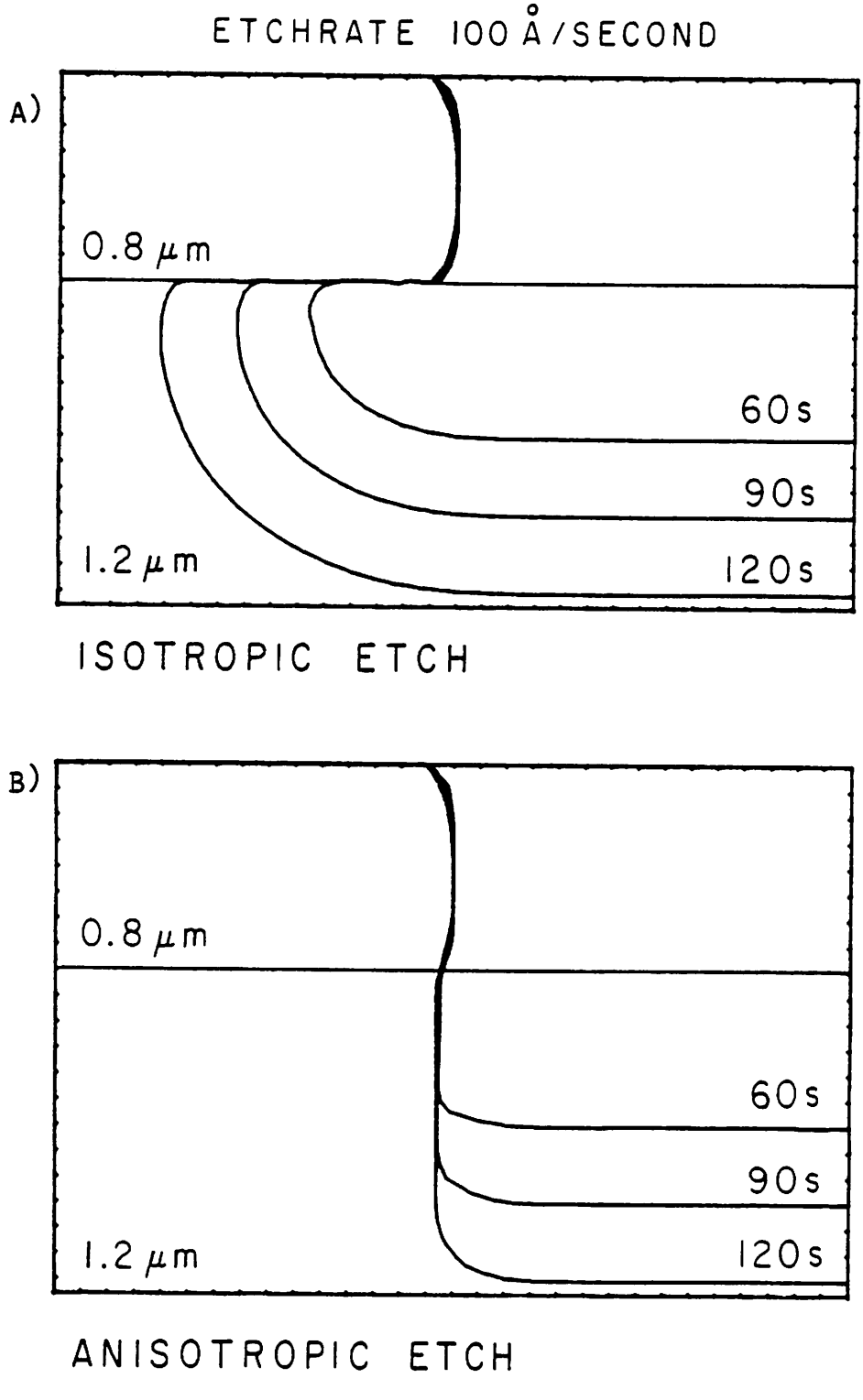
ETCHRATE 100 Å/SECOND
A)
0.8 μm
60s
90s
1.2 μm
120s
ISOTROPIC ETCH
B)
0.8 μm
60s
90s
1.2 μm
120s
ANISOTROPIC ETCH

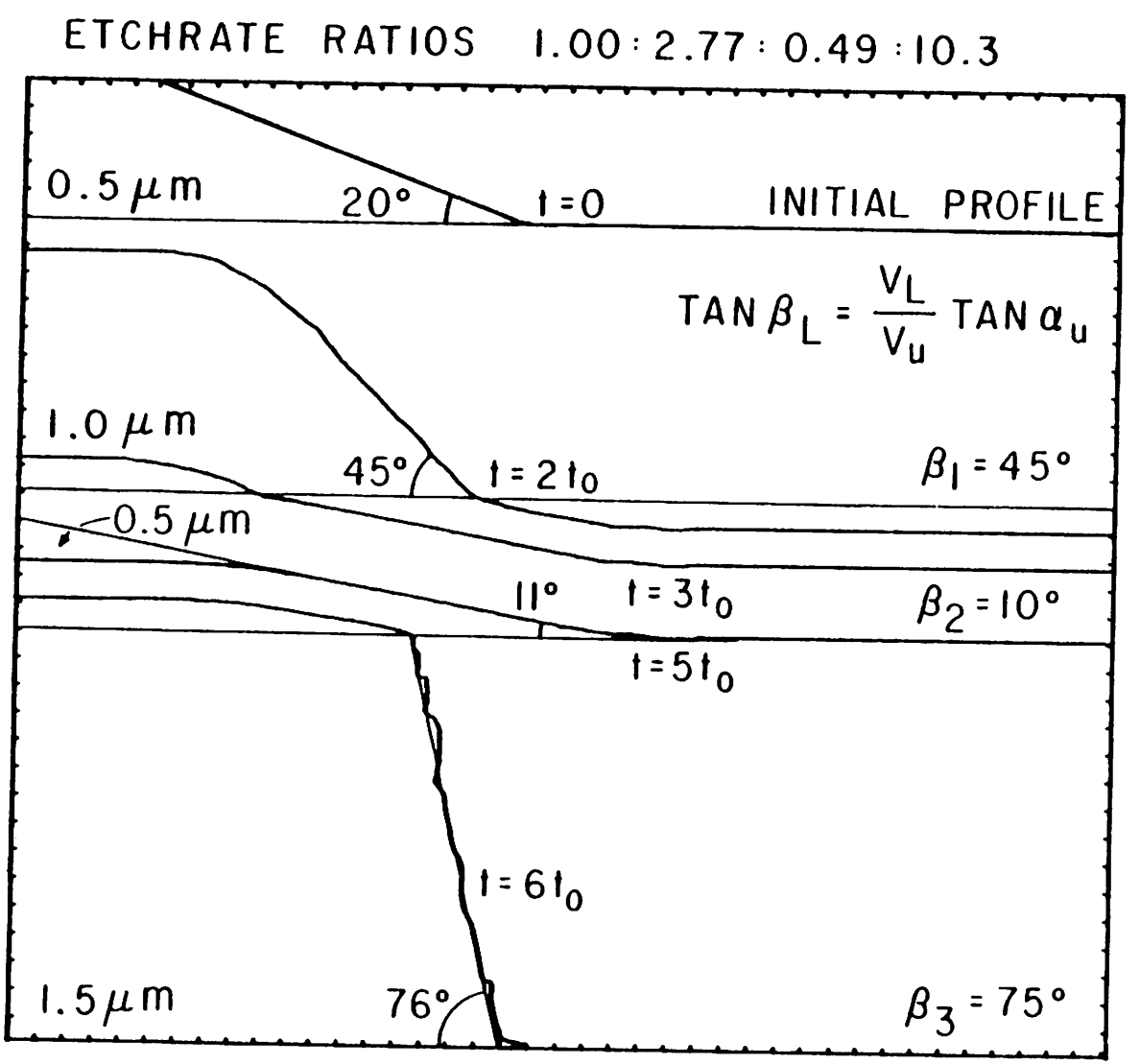

FIGURE 8: COMPUTER SIMULATION AND ANALYTICAL SOLUTION

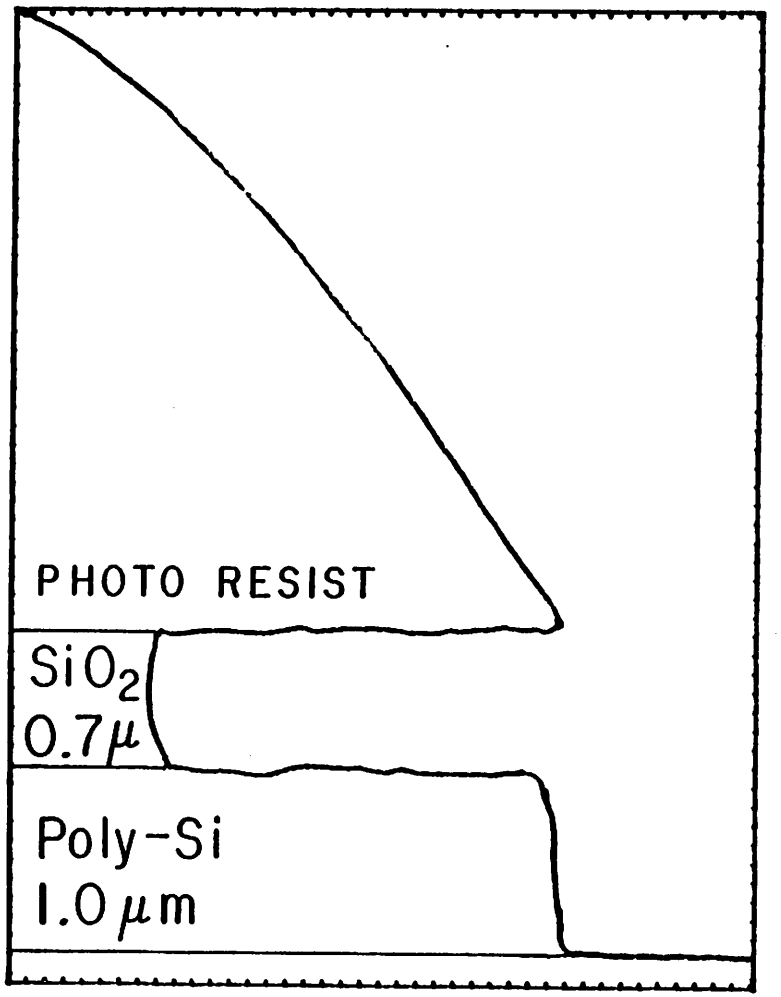

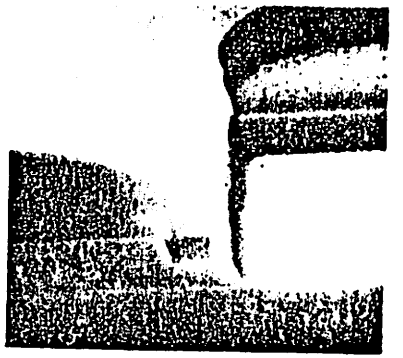

Mogab & Harsh-
barger, Electronics,
August 31, 1978

ISOTROPIC UNDERCUT FOLLOWED BY
ANISOTROPIC ETCH

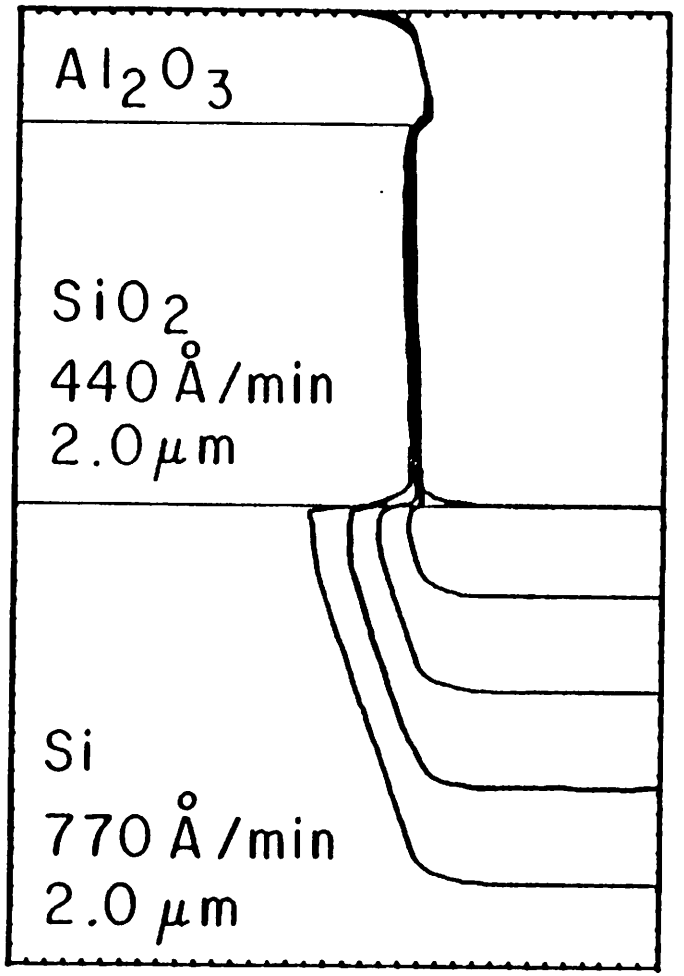

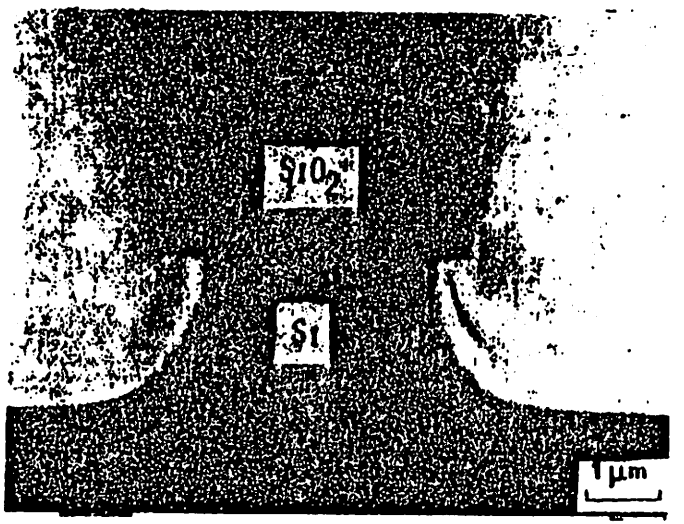

Schwartz, Rothman, & Schopen, J. Electrochem. Soc. Vol. 126, 3 (March 1979)

REACTIVE ION ETCHING OF SiO_2 ON Si

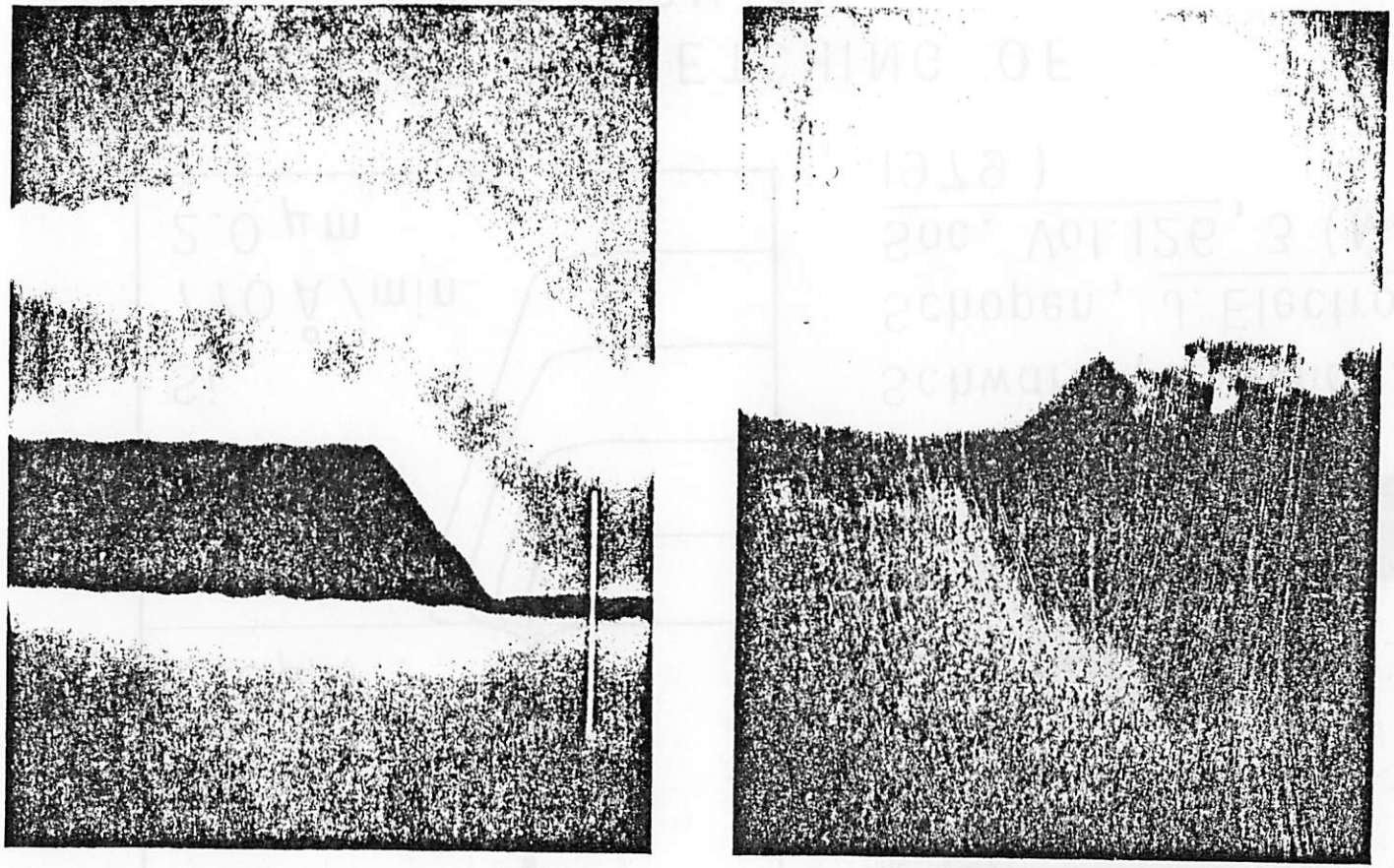

REACTIVE ION ETCH OF POLY-Si (0.5μm)
DEPOSITED OVER SiO_2 STEP

FIGURE 12.

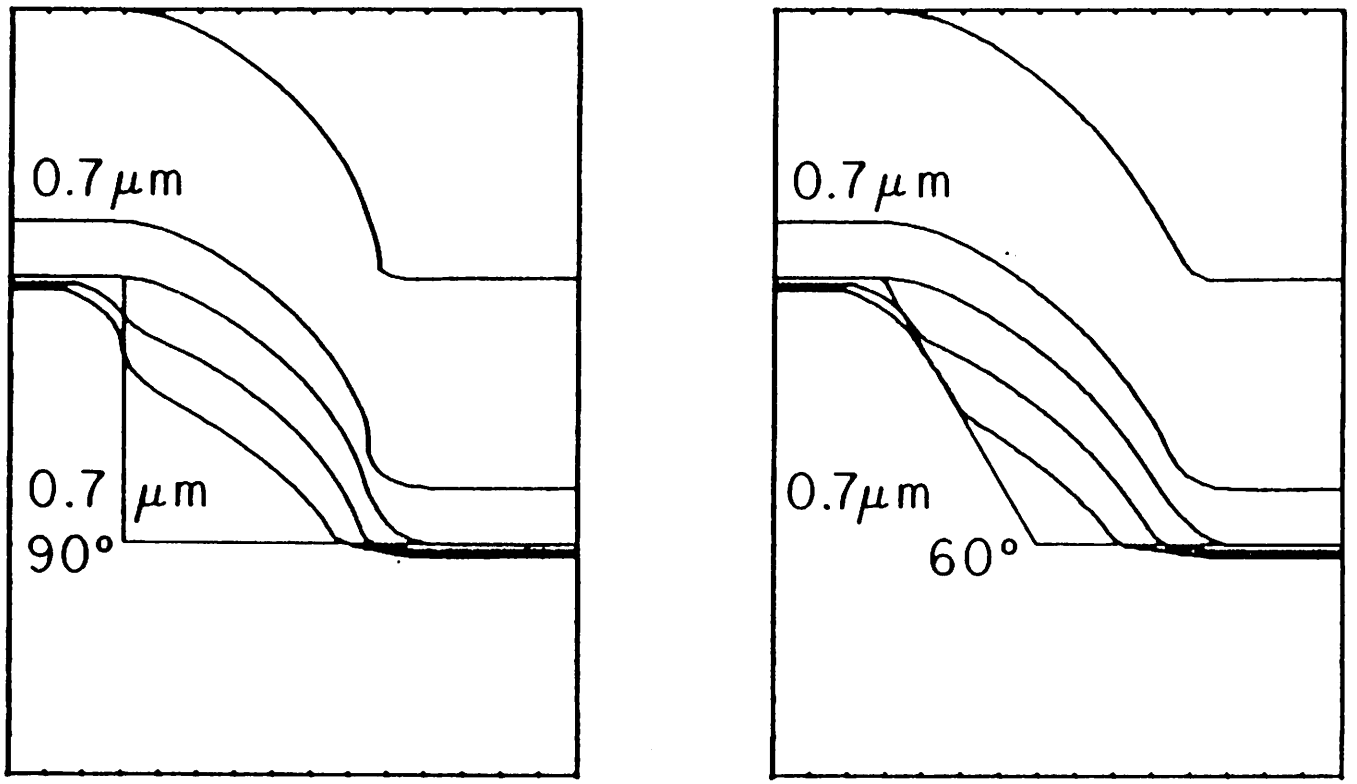

ISOTROPIC DEPOSITION FOLLOWED BY ANISOTROPIC ETCHING

FIGURE 12 (CON'T).

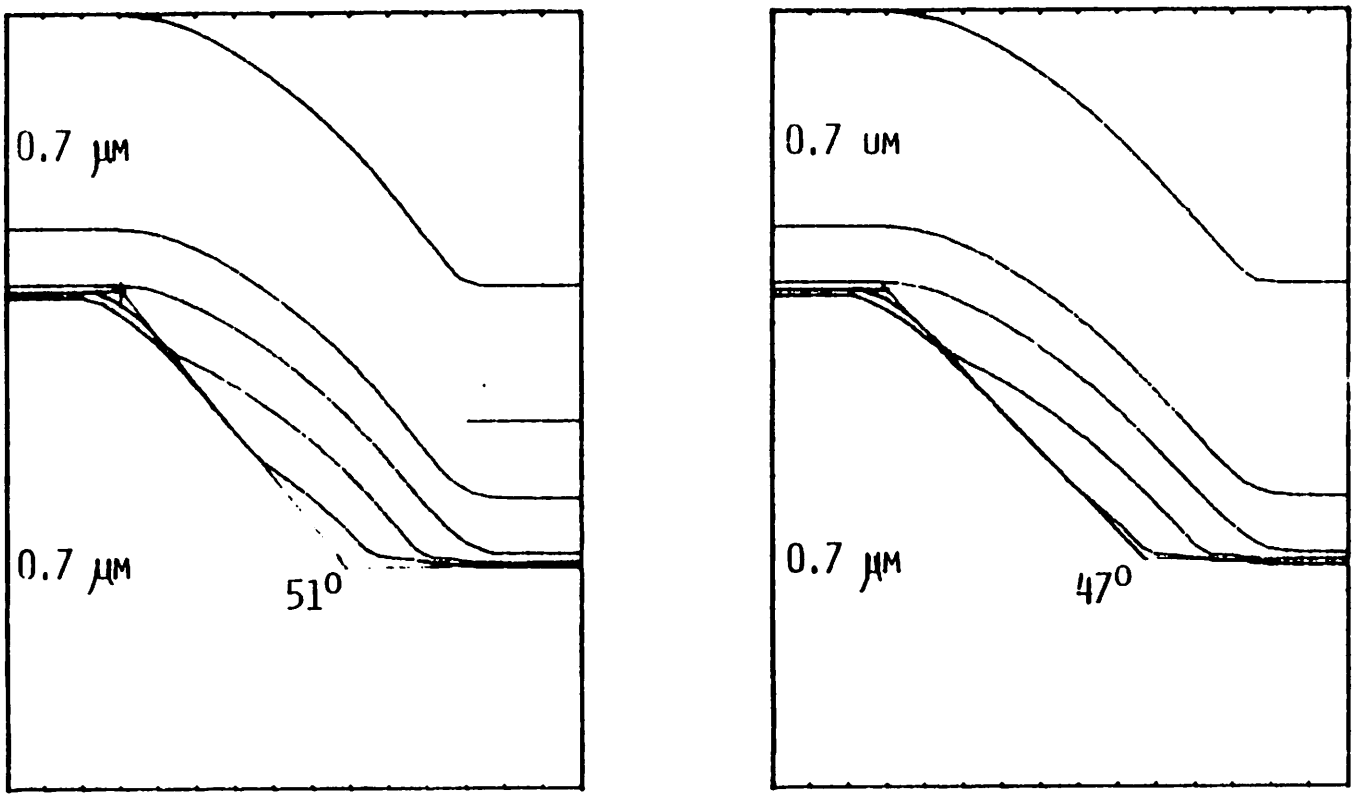

ISOTROPIC DEPOSITION FOLLOWED BY
ANISOTROPIC ETCHING

FIGURE 12 (CON'T).

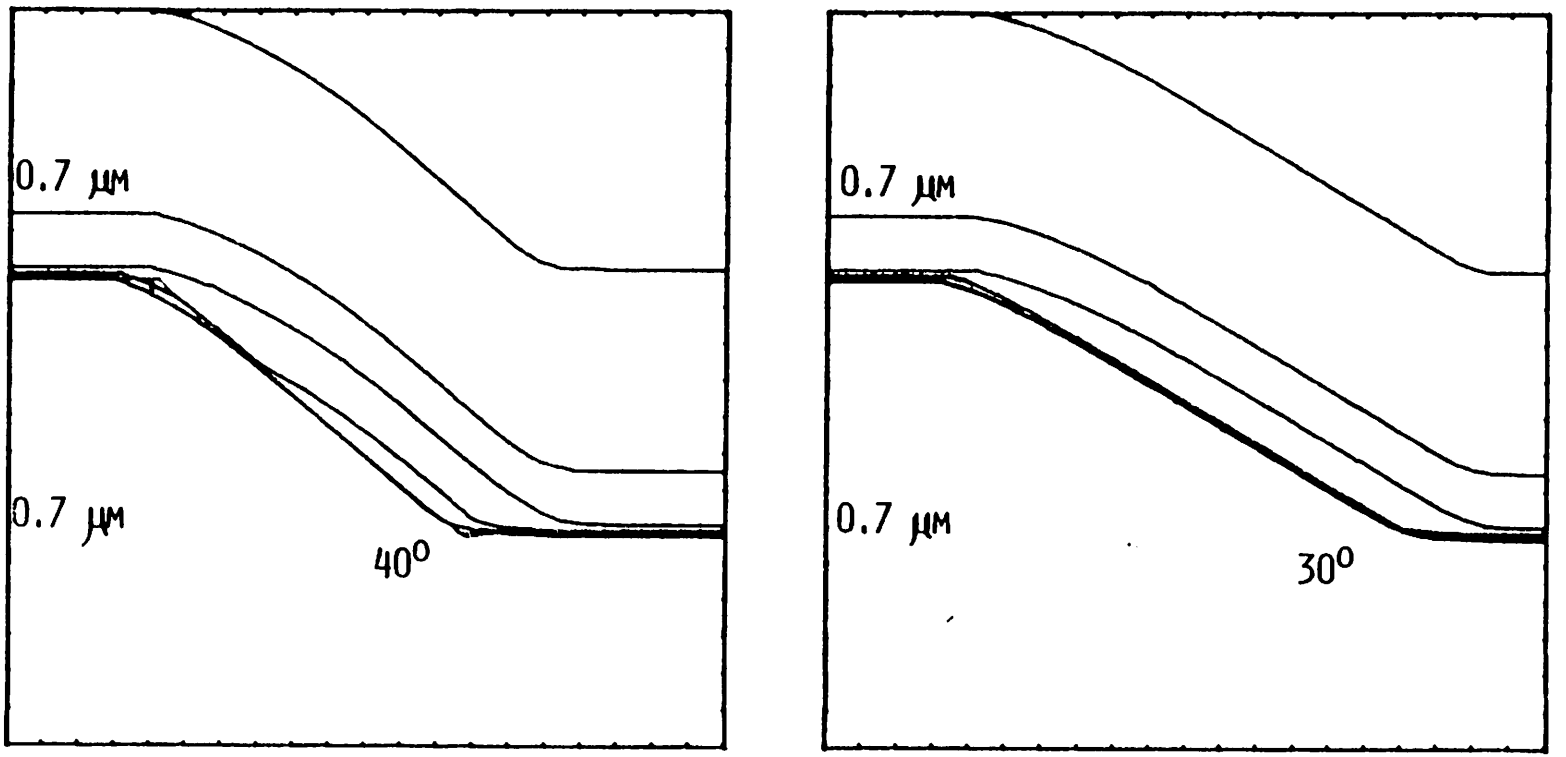

ISOTROPIC DEPOSITION FOLLOWED BY
ANISOTROPIC ETCHING

FIGURE 12 (CON'T): ISOTROPIC DEPOSITION FOLLOWED BY ANISOTROPIC ETCHING

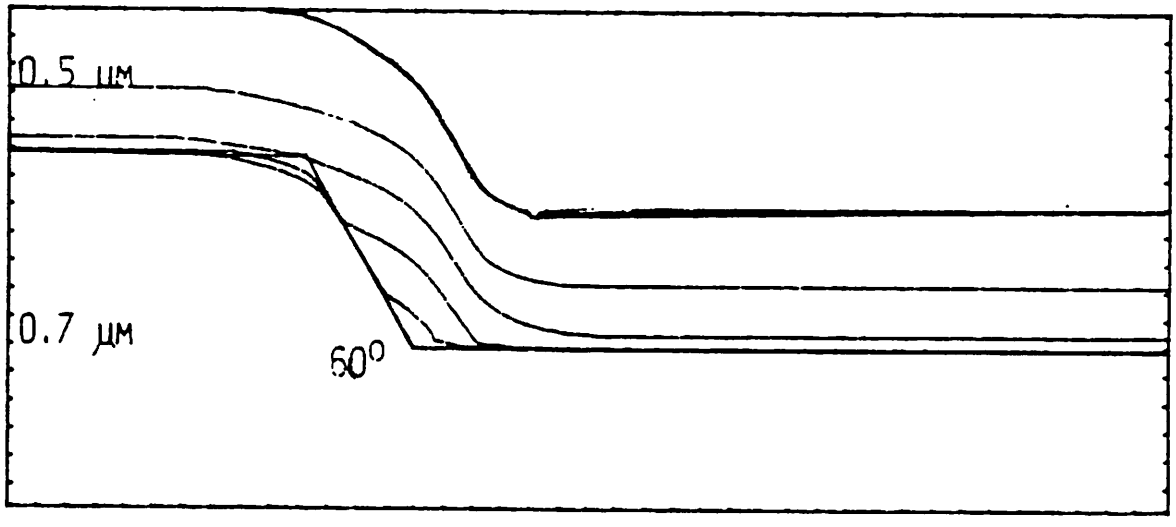

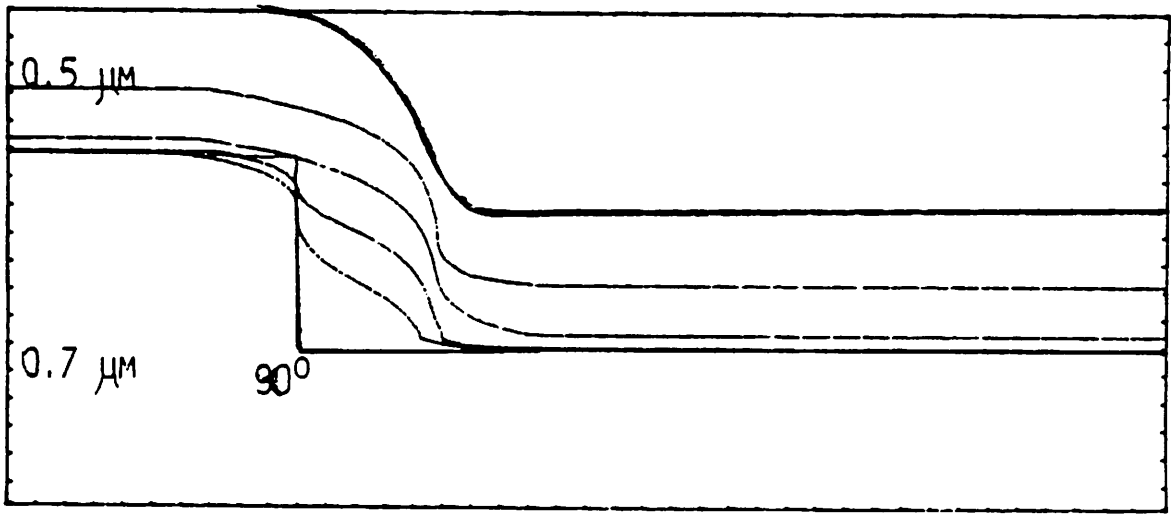

FIGURE 12 (CON'T).

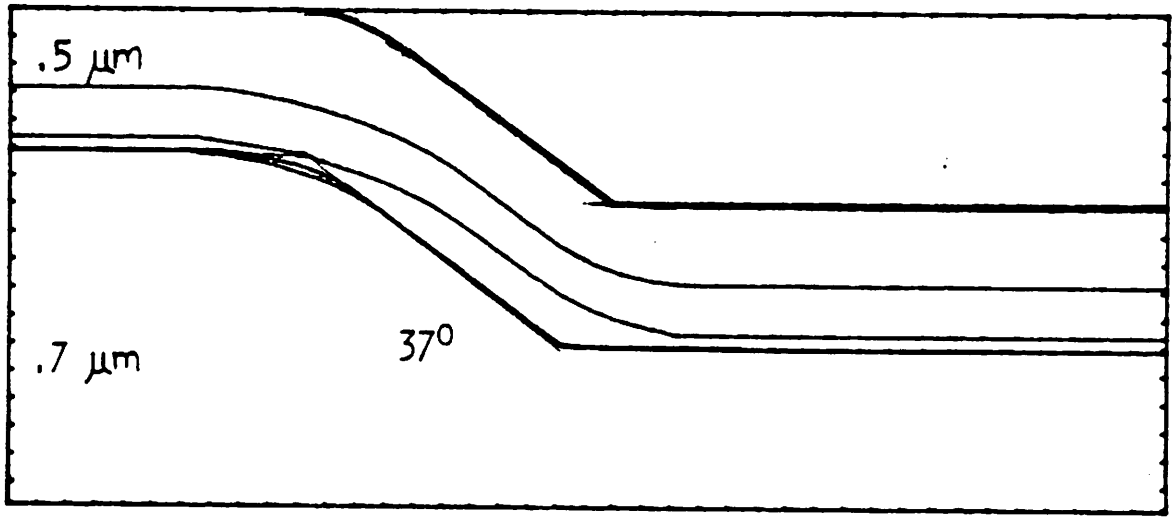

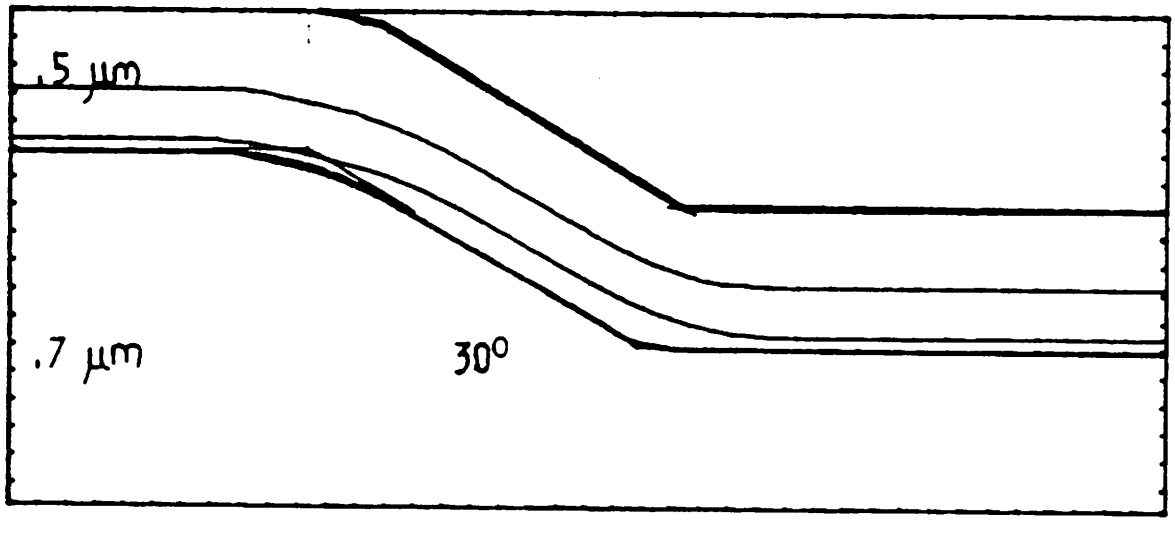

ISOTROPIC DEPOSITION FOLLOWED BY
ANISOTROPIC ETCH

FIGURE 12 (CON'T).

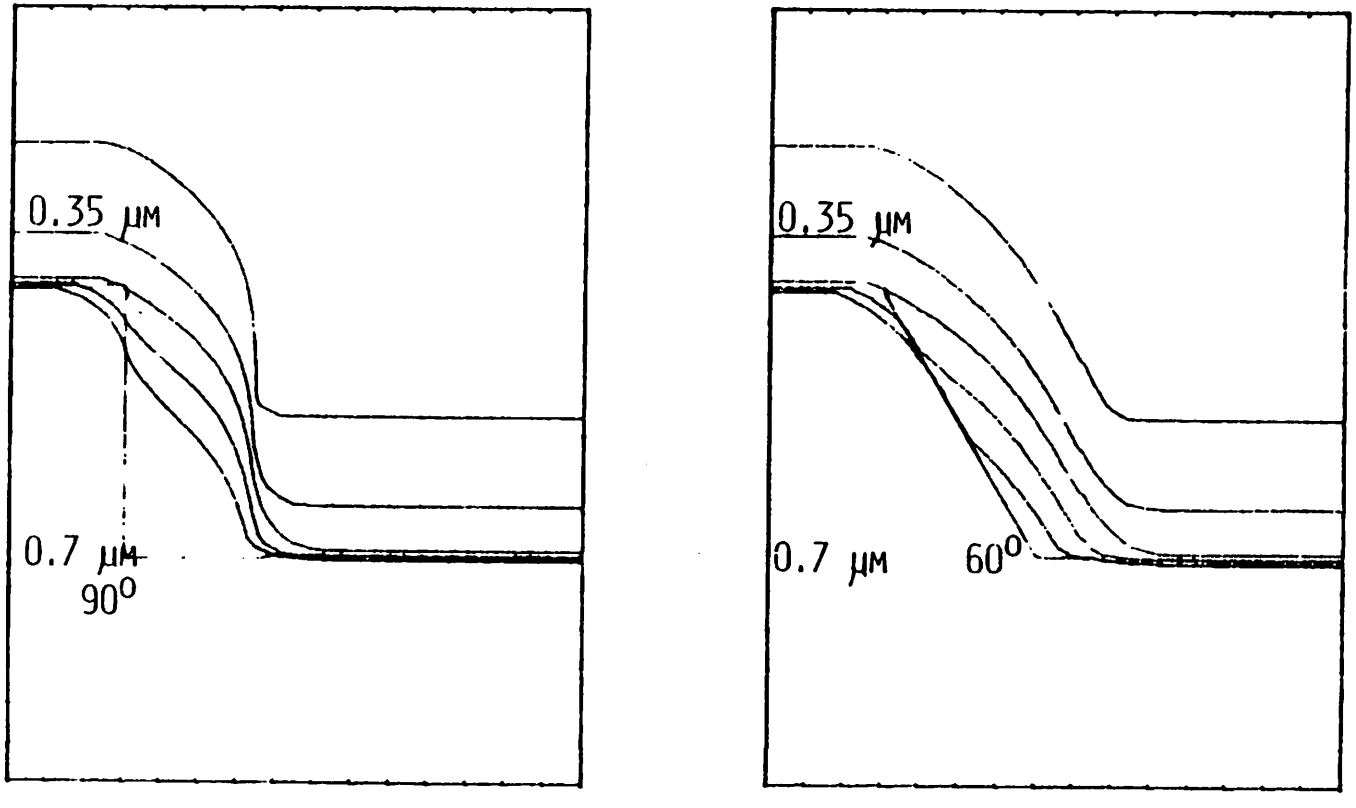

ISOTROPIC DEPOSITION FOLLOWED BY
ANISOTROPIC ETCHING

FIGURE 12 (CON'T)

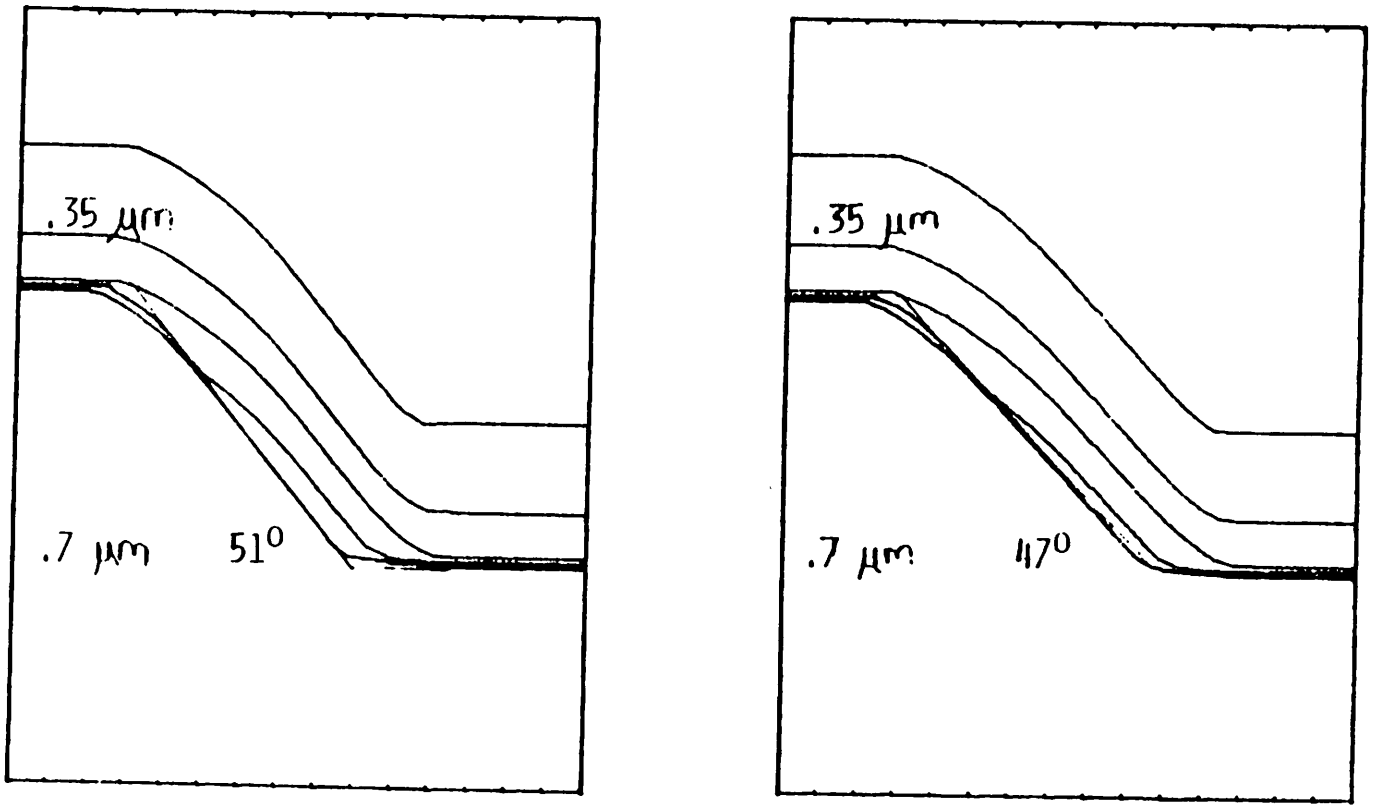

ISOTROPIC DEPOSTITION FOLLOWED BY ANISOTROPIC ETCH

FIGURE 12 (CON'T).

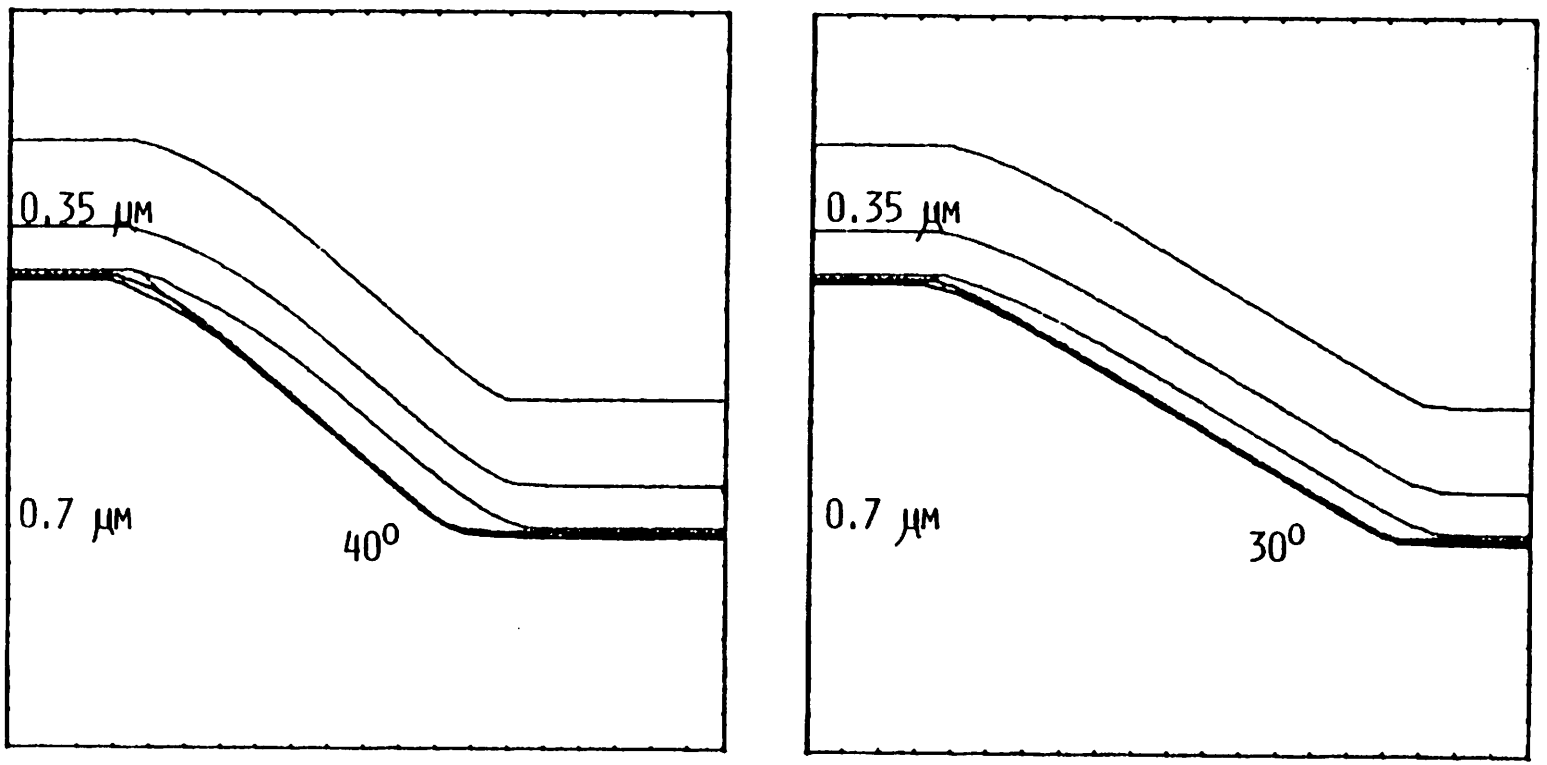

ISOTROPIC DEPOSITION FOLLOWED BY
ANISOTROPIC ETCHING

FIGURE 13.

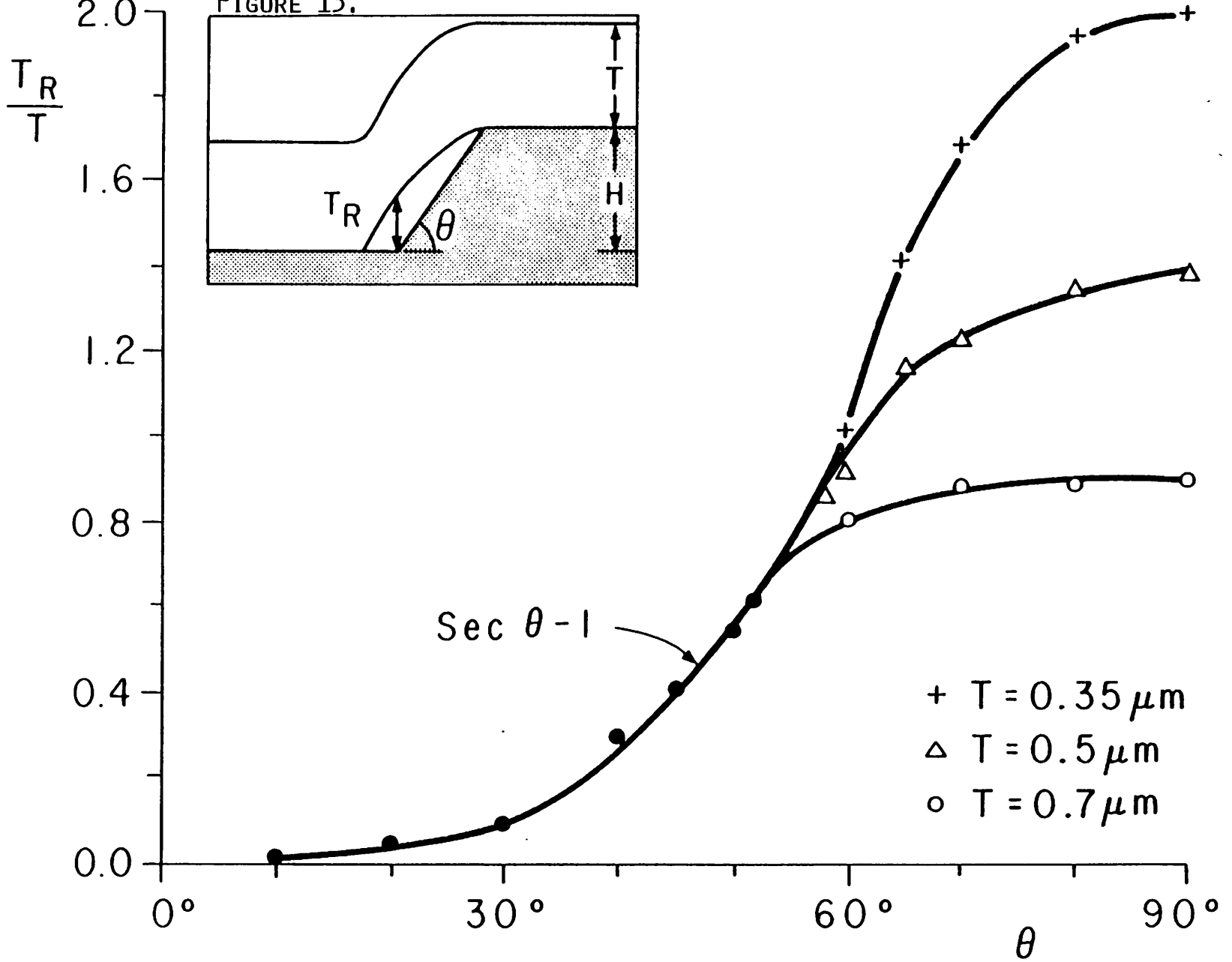

NORMALIZED RESIDUE VERSUS STEP TAPER

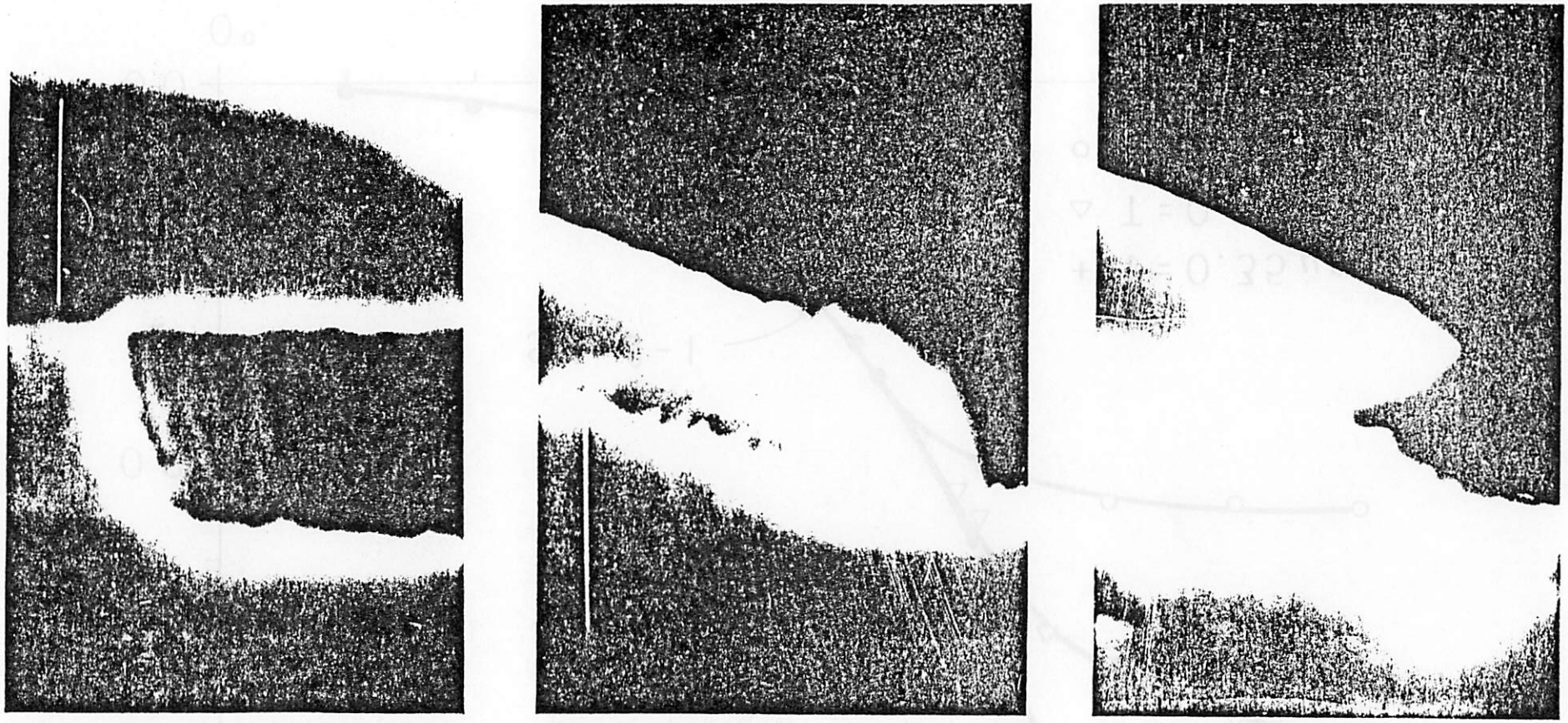

NO IMPLANT $5 \times 10^{14}/cm^2$ $10^{15}/cm^2$

PLASMA ETCHED PROFILES FOR As IM-PLANTED SURFACE LAYERS

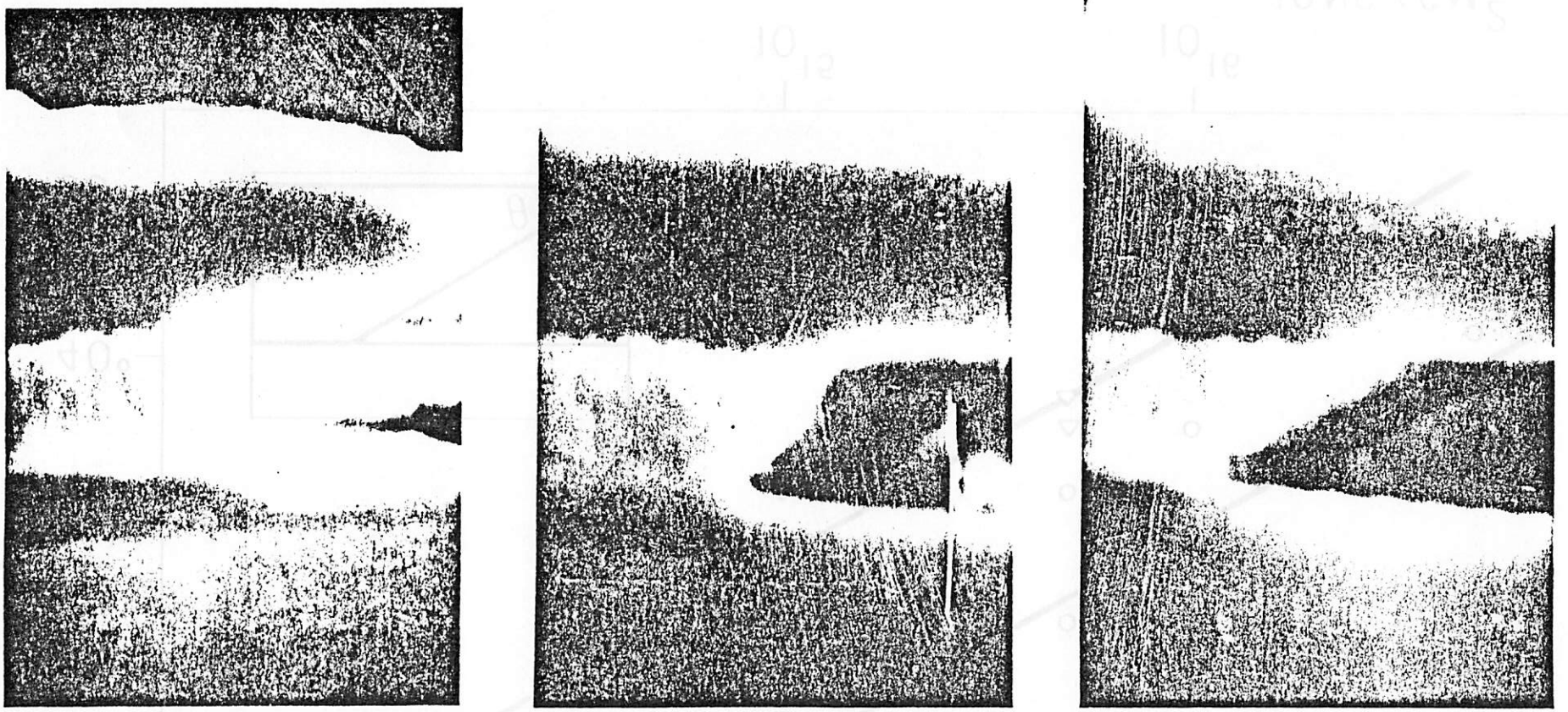

NO IMPLANT 5×10^{14} 5×10^{16}

PLASMA ETCHED PROFILES FOR As IM-PLANTED BURIED LAYERS

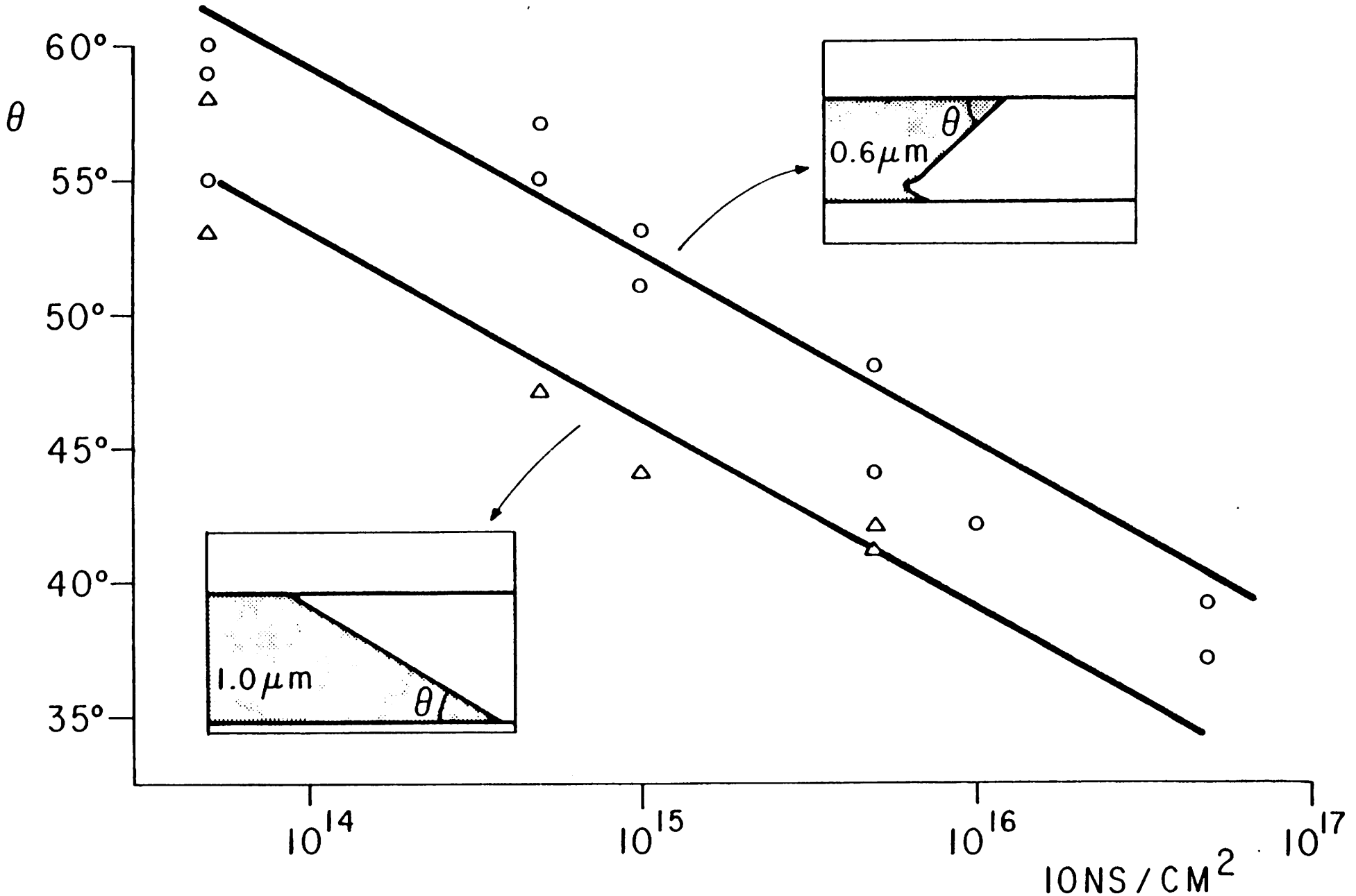

FIGURE 16.

PROFILE ANGLE VERSUS IMPLANT DOSE

FIGURE 17.

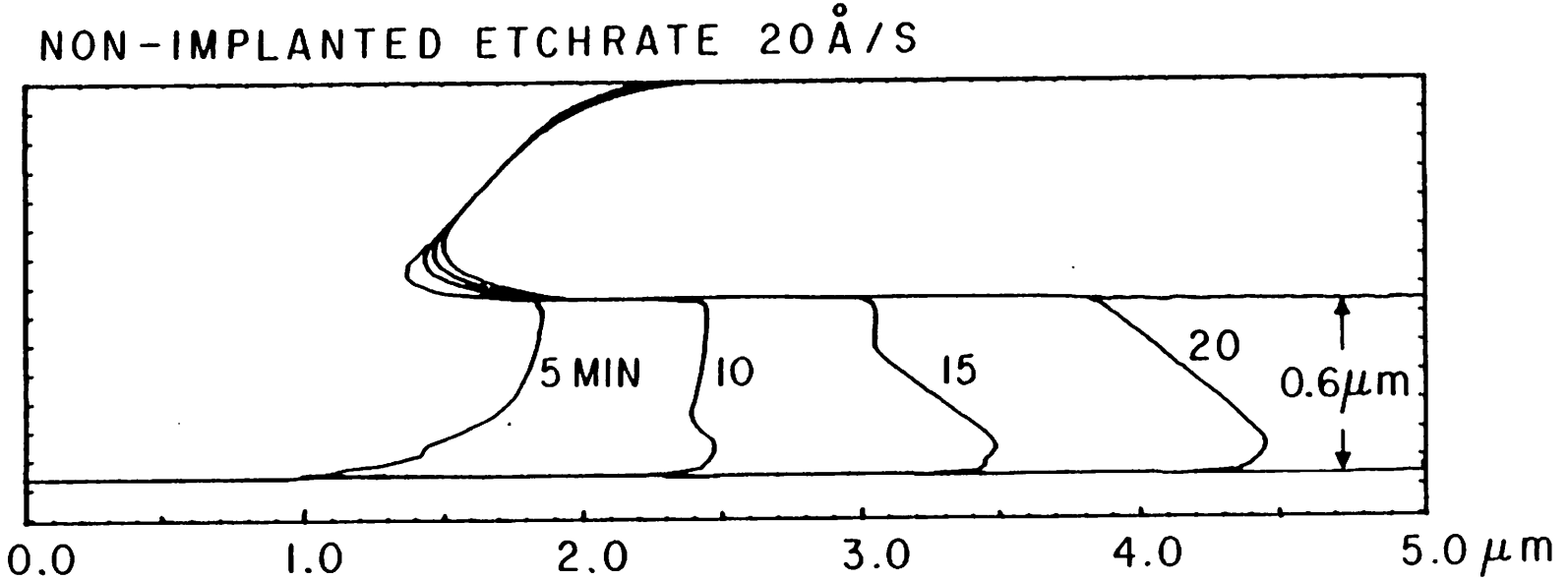

SIMULATION OF BURIED LAYER IMPLANT AND PLASMA ETCH

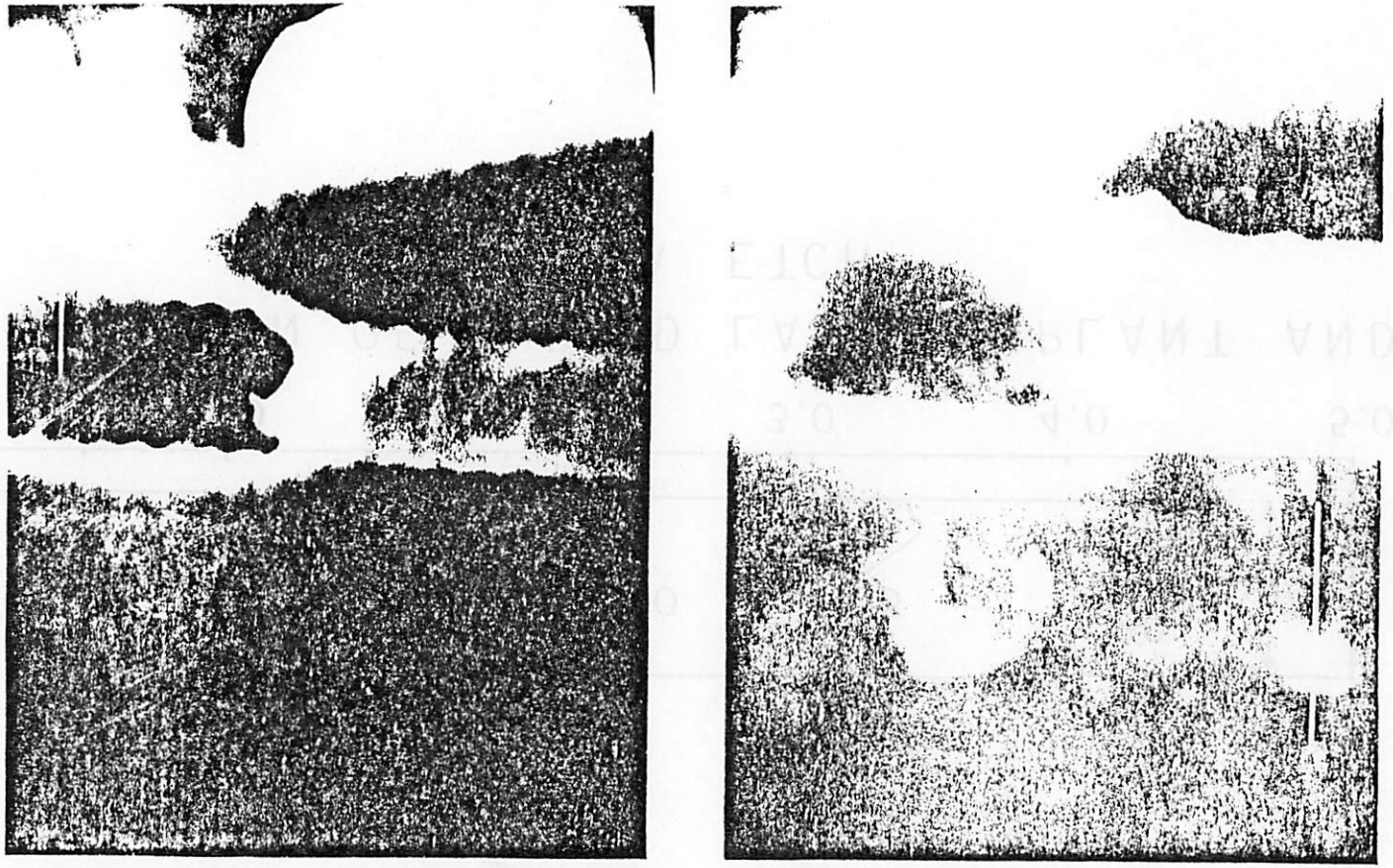

15 min

30 min

PROFILE EVOLUTION OF AS IMPLANTED BURIED LAYER

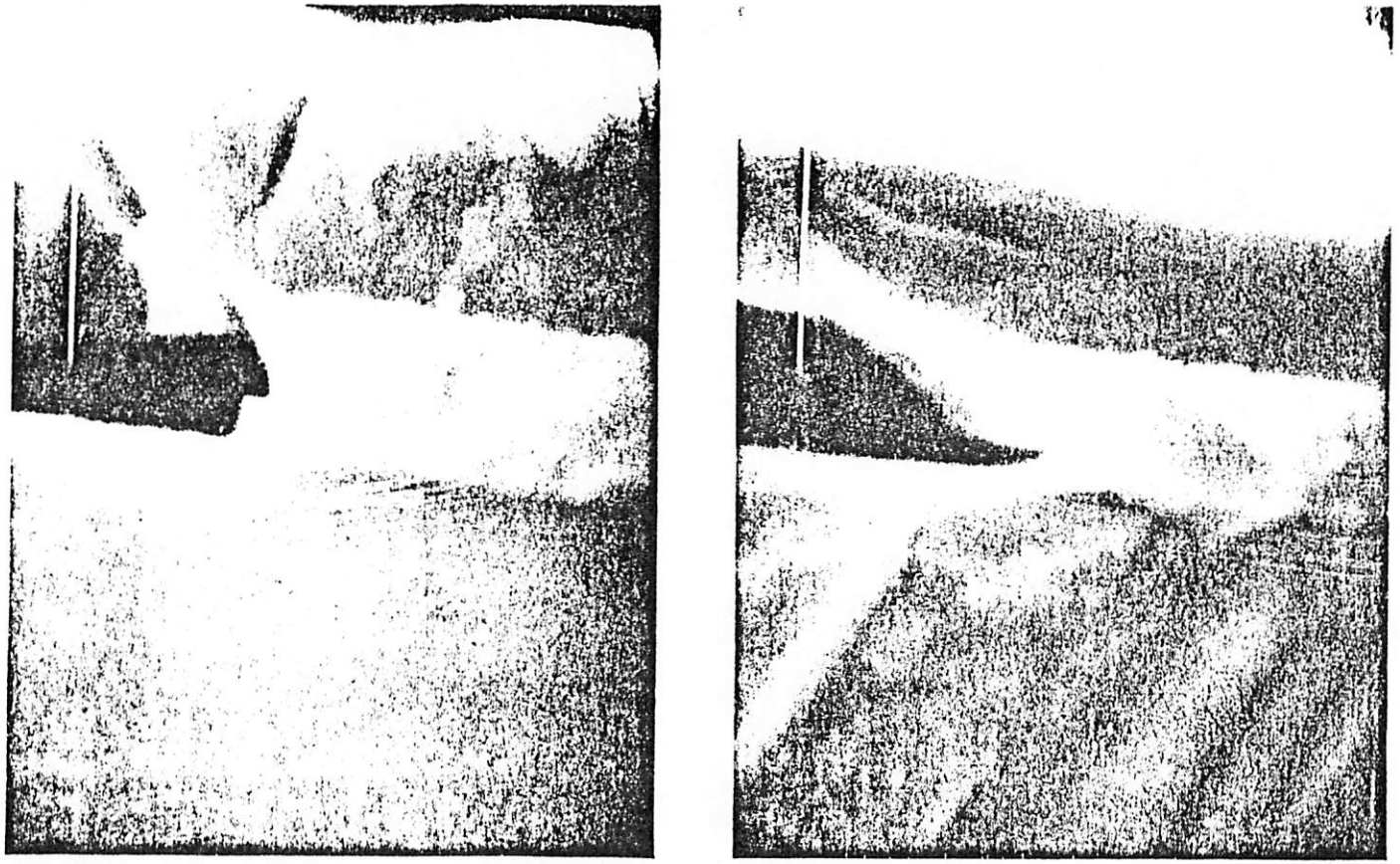

$5 \times 10^{13}/cm^2$ $10^{16}/cm^2$

ANOMALIES IN AS IMPLANTED
BURIED LAYERS